AD-A159 114 DLTS (DEEP-LEVEL TRANSIENT SPECTROSCOPY) ANALYSIS OF GERMANIUM AND AL SUB.. (U) UNIVERSAL ENERGY SYSTEMS INC DAYTON OH S S LI JUL 85 AFWAL-TR-84-2093 1/1

UNCLASSIFIED F33615-81-C-2058 F/G 10/2 NL

END

FILMED

DTIC

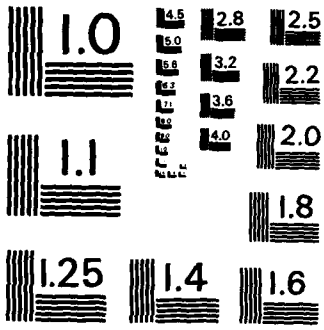

MICROCOPY RESOLUTION TEST CHART
NATIONAL BUREAU OF STANDARDS - 1963 - A

(2)

AD-A159 114

AFWAL-TR-84-2093

DLTS ANALYSIS OF GERMANIUM AND $Al_xGa_{1-x}As$ SOLAR CELLS

Sheng S. Li
UNIVERSITY OF FLORIDA
GAINESVILLE, FLORIDA 32611

JULY 1985

FINAL REPORT FOR PERIOD MARCH 1984 - SEPTEMBER 1984

APPROVED FOR PUBLIC RELEASE; DISTRIBUTION UNLIMITED.

DTIC FILE COPY

DTIC
ELECTE
SEP 1 7 1985
S D

AERO PROPULSION LABORATORY
AIR FORCE WRIGHT AERONAUTICAL LABORATORIES
AIR FORCE SYSTEMS COMMAND
WRIGHT-PATTERSON AIR FORCE BASE, OHIO 45433

85 9 13 039

NOTICE

When Government drawings, specifications, or other data are used for any purpose other than in connection with a definitely related Government procurement operation, the United States Government thereby incurs no responsibility nor any obligation whatsoever; and the fact that the government may have formulated, furnished, or in any way supplied the said drawings, specifications, or other data, is not to be regarded by implication or otherwise as in any manner licensing the holder or any other person or corporation, or conveying any rights or permission to manufacture, use, or sell any patented invention that may in any way be related thereto.

This report has been reviewed by the Information Office (OI) and is releasable to the National Technical Information Service (NTIS). At NTIS, it will be available to the general public, including foreign nations.

This technical report has been reviewed and is approved for publication.

W. PATRICK RAHILLY
Project Engineer

PAUL R. BERTHEAUD
Chief, Power Components Branch

FOR THE COMMANDER

JAMES D. REAMS
Chief, Aerospace Power Division
Aero Propulsion Laboratory

"If your address has changed, if you wish to be removed from our mailing list, or if the addressee is no longer employed by your organization please notify AFWAL/POOC *, W-PAFB, OH 45433 to help us maintain a current mailing list".*

Copies of this report should not be returned unless return is required by security considerations, contractual obligations, or notice on a specific document.

Unclassified
SECURITY CLASSIFICATION OF THIS PAGE

A159114

REPORT DOCUMENTATION PAGE

1a. REPORT SECURITY CLASSIFICATION Unclassified	1b. RESTRICTIVE MARKINGS
2a. SECURITY CLASSIFICATION AUTHORITY 2b. DECLASSIFICATION/DOWNGRADING SCHEDULE	3. DISTRIBUTION/AVAILABILITY OF REPORT Approved for public release; distribution unlimited.
4. PERFORMING ORGANIZATION REPORT NUMBER(S)	5. MONITORING ORGANIZATION REPORT NUMBER(S) AFWAL-TR-84-2093
6a. NAME OF PERFORMING ORGANIZATION University of Florida 6b. OFFICE SYMBOL (If applicable)	7a. NAME OF MONITORING ORGANIZATION Aero Propulsion Laboratory (AFWAL/POOC) AF Wright Aeronautical Laboratories (AFSC)
6c. ADDRESS (City, State and ZIP Code) Gainesville Florida 32611	7b. ADDRESS (City, State and ZIP Code) Wright-Patterson Air Force Base, Ohio 45433
8a. NAME OF FUNDING/SPONSORING ORGANIZATION Universal Energy Systems 8b. OFFICE SYMBOL (If applicable)	9. PROCUREMENT INSTRUMENT IDENTIFICATION NUMBER F33615-81-C-2058
8c. ADDRESS (City, State and ZIP Code) 4401 Dayton-Xenia Road Dayton OH 45432	10. SOURCE OF FUNDING NOS. PROGRAM ELEMENT NO. 62203F; PROJECT NO. 3145; TASK NO. 19; WORK UNIT NO. 10
11. TITLE (Include Security Classification) DLTS Analysis of Germanium and AlGaAs As Solar Cells	
12. PERSONAL AUTHOR(S) Sheng S. Li	
13a. TYPE OF REPORT Final 13b. TIME COVERED FROM March 84 TO Sep 84	14. DATE OF REPORT (Yr., Mo., Day) 85 July 15. PAGE COUNT 64
16. SUPPLEMENTARY NOTATION This effort was accomplished under the AFWAL/POO Scholarly Research Program	

17. COSATI CODES			18. SUBJECT TERMS (Continue on reverse if necessary and identify by block number)
FIELD	GROUP	SUB. GR.	DLTS III-V SOLAR CELLS RADIATION DEFECTS
1001	2202	2012	

19. ABSTRACT (Continue on reverse if necessary and identify by block number)

Radiation-induced deep-level defects in one-MeV electron irradiated germanium and AlGaAs were analyzed with DLTS and with capacitance-voltage techniques. The defect rate is independent of total fluence but depends on the doping density. The traps are vacancy plus impurity complexes. Germanium cells show strong radiation resist. In AlGaAs, irradiation caused some increase in density of two native defects while no new deep-level defects were found.

20. DISTRIBUTION/AVAILABILITY OF ABSTRACT UNCLASSIFIED/UNLIMITED ☒ SAME AS RPT. ☐ DTIC USERS ☐	21. ABSTRACT SECURITY CLASSIFICATION Unclassified
22a. NAME OF RESPONSIBLE INDIVIDUAL W. PATRICK RAHILLY	22b. TELEPHONE NUMBER (Include Area Code) (513)255-6235 22c. OFFICE SYMBOL AFWAL/POOC

DD FORM 1473, 83 APR EDITION OF 1 JAN 73 IS OBSOLETE.

Unclassified
SECURITY CLASSIFICATION OF THIS PAGE

Table of Contents

page

I. Introduction 1

II. Radiation Induced Defects in Germanium and $Al_xGa_{1-x}As$ 1

III. Results of One-MeV Electron Irradiation in Germanium 3

IV. Results of One-MeV Electron Irradiation in $Al_xGa_{1-x}As$ 52

V. Conclusions 57

VI. References 61

VII. Publications and Conference Presentations 62

Accession For
NTIS GRA&I ☒
DTIC TAB ☐
Unannounced ☐
Justification
By
Distribution/
Availability Codes
Dist | Avail and/or Special
A-1

DTIC COPY INSPECTED 6

I. Introduction

The objective of this research project is to investigate the radiation-induced deep-level defects in the one-MeV electron irradiated germanium and $Al_xGa_{1-x}As$ with x=0.05 and 0.17 using the Deep-Level Transient Spectroscopy (DLTS) and Capacitance - Voltage (C-V) techniques. The I-V and C-V measurements were employed to estimate the background concentration in Ge irradiated by the one-MeV electrons for fluences of $1x10^{14}$, $1x10^{15}$, $1x10^{16}$ cm^{-2} and in $Al_xGa_{1-x}As$ for fluences of $1x10^{15}$ and $1x10^{16}$. The C-V and DLTS measurements were used to determine the defect parameters such as energy level, defect density and capture cross section of both electron and hole traps. This information is vital for designing a radiation hard cascade solar cell using materials such as germanium, GaAs and $Al_xGa_{1-x}As$.

Section II provides a brief overview of the radiation induced defects in germanium and AlGaAs as reported in the literature. In section III the results of the I-V, C-V and DLTS measurements on germanium samples are discussed. The physical origin of the radiation-induced defects are also depicted. Section VI described the DLTS and C-V results for the $Al_xGa_{1-x}As$ (with x = 0.05 and 0.17) specimen. Conclusions are given in the section V. Section VI lists the references.

II. Radiation Induced Defects in Germanium and $Al_xGa_{1-x}As$

2.1 Germanium

The high energy electron irradiation usually introduces vacancies and interstitials in germanium. The defects created by the room temperature irradiation are normally referred to as the secondary defects which are different from the primary defects generated in low-temperature irradiation such as vacancy-interstitial pairs. The major defects induced by irradiation are explained as follows:

Deep-level defects induced in n-type germanium irradiated by high energy electrons or gamma ray, are due to acceptor type vacancy related complex. It is commonly known that one acceptor level around E_c- 0.2 eV and a deeper acceptor level below the midgap were found in the electron irradiated germanium specimen. The concentration of these two acceptor levels are essentially the same [Reference 1]. It is noted that the E_v+ 0.17 eV hole trap level has been neglected in the literature, while Curtis predicted the existence of a hole trap level around 0.17 eV above the valence band [Reference 2].

The physical origin of the E_c- 0.2 eV (including the E_c- 0.24 and E_c- 0.27 eV) is ascribed to the vacancy-substitutional impurity complex. The E_v+ 0.1 eV is a divacancy-substitutional impurity complex [References 3-5]. The defect introduction rate for these defects is independent of the electron fluence but is dependent upon the doping impurity. Thus, it is believed that these defects are likely to be impurity related.

The E_v+ 0.17 eV hole trap observed in the germanium samples studied here, is attributed to a divacancy-interstitial impurity complex. This will be explained further in section 3-3.

2.2 $Al_xGa_{1-x}As$ Epitaxial Materials

No detectable deep-level defects was observed in $Al_xGa_{1-x}As$ samples with x = 0.05, while two electron traps with energies of E_c- 0.19 eV and E_c- 0.29 eV where observed in samples with x = 0.17. However, these two electron traps were also observed in the unirradiated AlGaAs samples. Thus, they are believed to be associated with the grown-in native defects and not the irradiation-induced defects. Since they are not dependending on the doping density and electron fluence, these two electron traps are not related to impurities.

In the next section, we shall present the results of our DLTS analysis of the radiation induced deep-level defects in germainum and AlGaAs samples. Both materials are potentially useful for cascade solar cell applications.

III. Results of One-MeV Electron Irradiation in Germanium

3.1 I-V measurements

The current - voltage (I-V) relationship under forward bias condition can be expressed by

$$J_F = q(D_p/\tau_p)^{1/2} n_i^2 N_D \exp(qV/kT) + q(W/2\tau_o)\, n_i \exp(qV/2kT) \qquad (3.1)$$

The first term in Eq.(3.1) is the diffusion current component, and the second term is due to the recombination current component. The empirical formula for the current density under forward bias can be represented by

$$J_F = A \exp(qV/nkT), \qquad 1 \leq n \leq 2 \qquad (3.2)$$

From our DLTS results, we have found that the unirradiated germanium samples used in the present study have a very high concentration of copper impurity (which has the $E_c - 0.26$ eV and $E_v + 0.33$ eV levels), their recombination current component was found to be quite high compared with the irradiated samples. The concentrations of the copper impurity were found to be $N_t = 2\times10^{15}$ cm^{-3} in samples with $N_D = 2\times10^{16}$ and $N_t = 4\times10^{14}$ in samples with $N_D = 10^{15}$ cm^{-3}. Copper can be easily found in germanium regardless of the types of doping material or methods of quenching used [Reference 11]. Fig. 3.1 and 3.2 show the forward I-V curves of germanium diodes studied in this work. The results show that values of recombination current do not increase significantly with increasing electron fluence in these germanium diodes. This result is consistent with our DLTS results in that no significant increase in defect density was observed in the electron irradiated germanium diodes when electron fluence is increased.

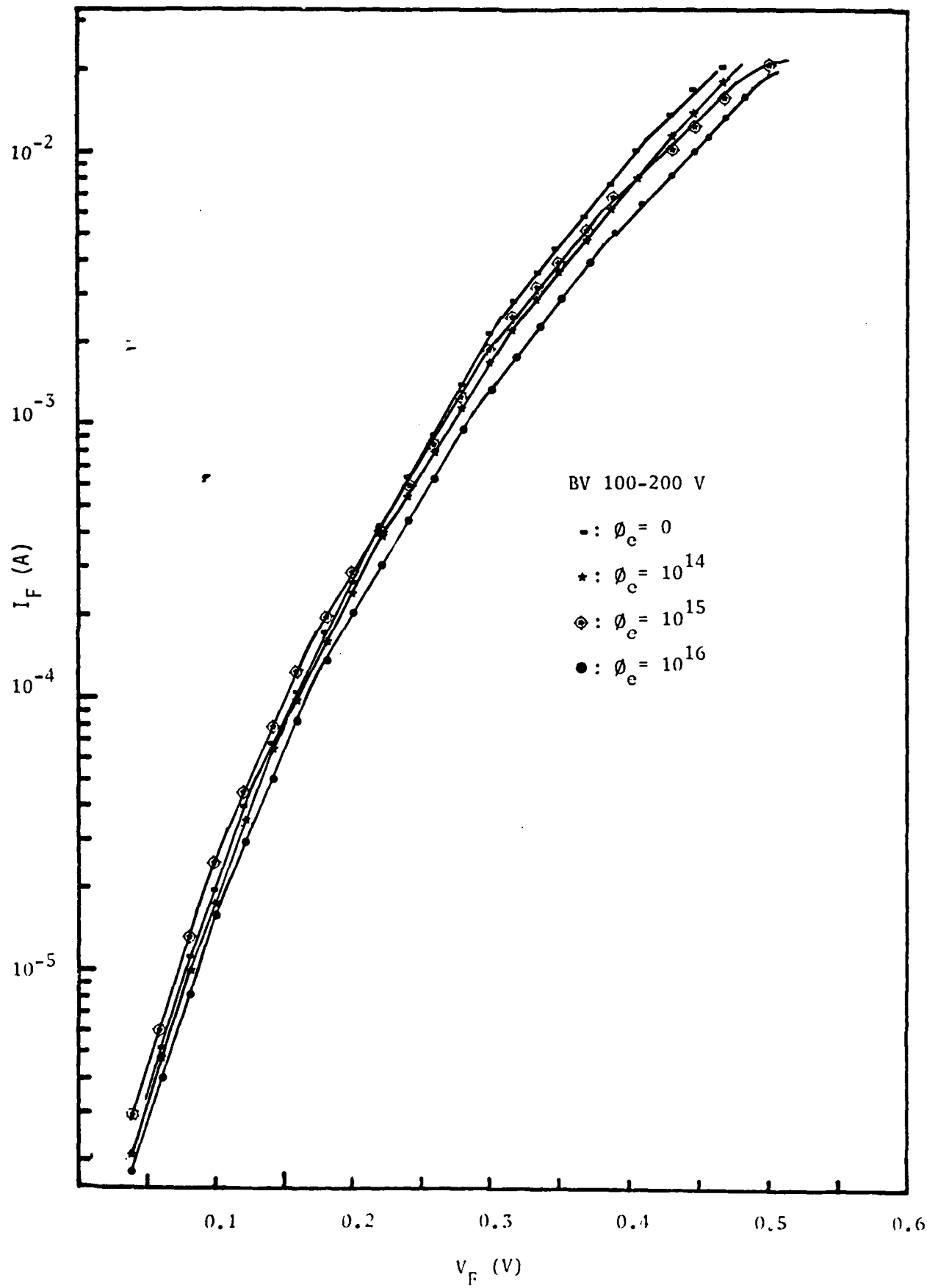

Fig. 3.1 Current versus forward-biased voltage in Germanium irradiated by One-MeV electron ($N_D = 10^{15}$).

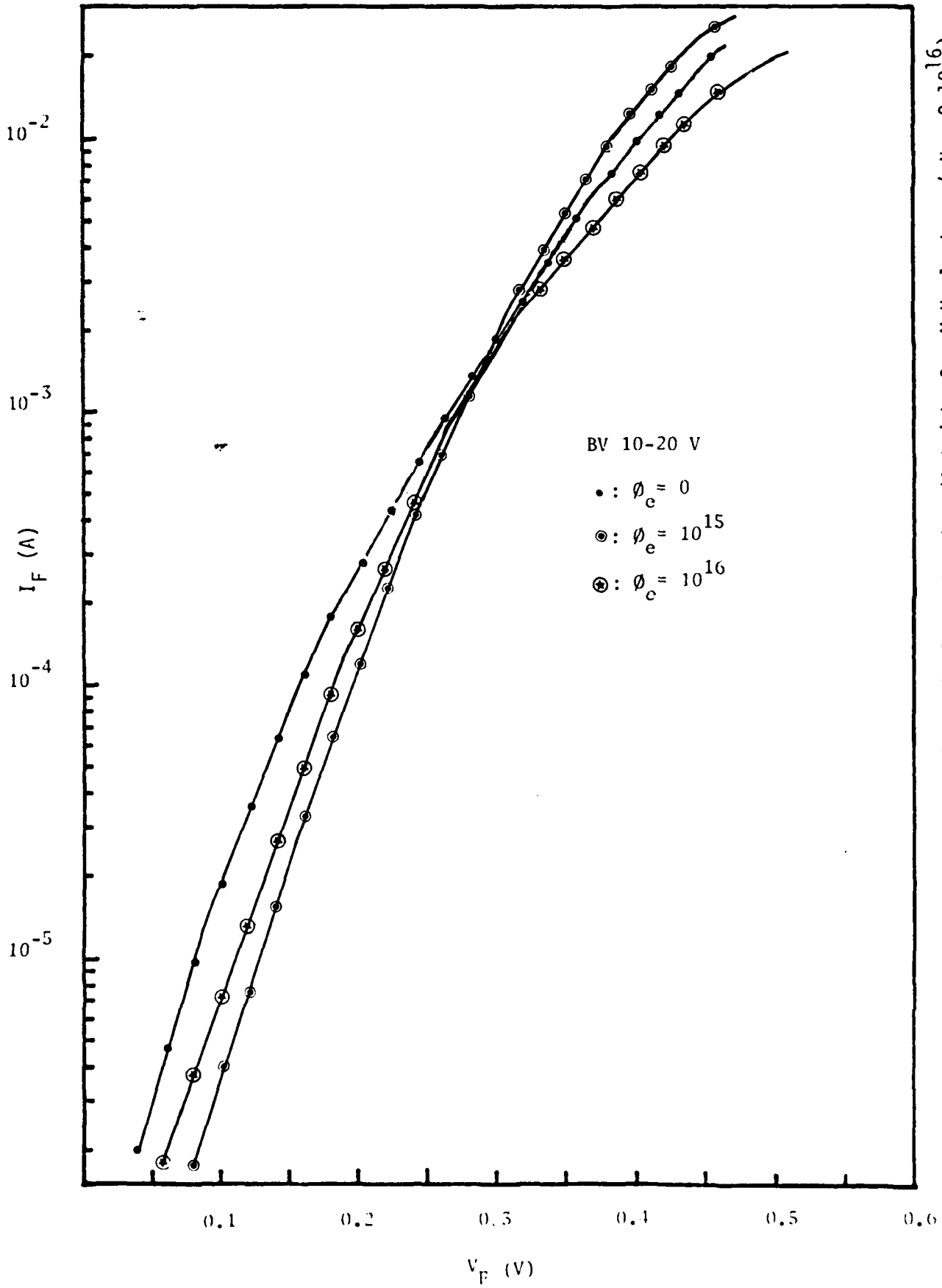

Fig. 3.2 Current vs forward-biased voltage in Germanium irradiated by One-MeV electron ($N_D = 2\times10^{16}$).

3.2 C-V measurements

From the C-V measurements the background dopant density can be determined by:

$$N_D = 2/q\epsilon_s \{ [- A^2/[d (1/C^2)/ dV] \} \qquad (3.3)$$

where A is the area of germanium diode. Note that these germanium samples are point contact diodes. Thus, it is difficult to measure the area accurately. To overcome this problem, we determine the diode area from the reverse breakdown voltage. Fig. 3.3 shows the breakdown voltage vs. impurity concentration for the one-sided abrupt junction germanium diode. Two groups of diodes with different breakdown voltages were used in this study. One group of diodes has a breakdown voltage between 100 and 200 V, and the other group of diodes has a breakdown voltage between 10 and 20 V. Accordingly, the ranges of background doping density are varied between 6.5×10^{14} and 1.5×10^{15} cm^{-3} for diodes with 100 to 200 V breakdown voltage, and between 1.2×10^{16} and $3.4 \times 10^{16} cm^{-3}$ for diodes with 10 to 20 V breakdown voltage, as predicted from the graph. The group with breakdown voltages between 100 and 200 V has a smaller estimated error of doping density if we assume $N_D = 10^{15}$ cm^{-3}. This result is in good agreement with our C-V measurements on the same diode in which a dopant density of approximately 10^{15} cm^{-3} was deduced from the C-V data. From the above analysis, the background doping density for the 100 to 200 V breakdown voltage diodes is assumed equal to 10^{15} cm^{-3} and the area of the diode is estimated to be $2.66 \times 10^{-5} cm^2$. The results of the measured C-V curves are shown in Fig. 3.4 and 3.5. In the germanium diodes with 10 to 20 V breakdown voltages, the background dopant density was calculated from the C-V curves for both the unirradiated and irradiated samples. The results yield a dopant density of $N_D = 2 \times 10^{16} cm^{-3}$ for diodes with 10-20 V breakdown voltage and $N_D = 1 \times 10^{15} cm^{-3}$ for diodes with 100 - 200 Volts

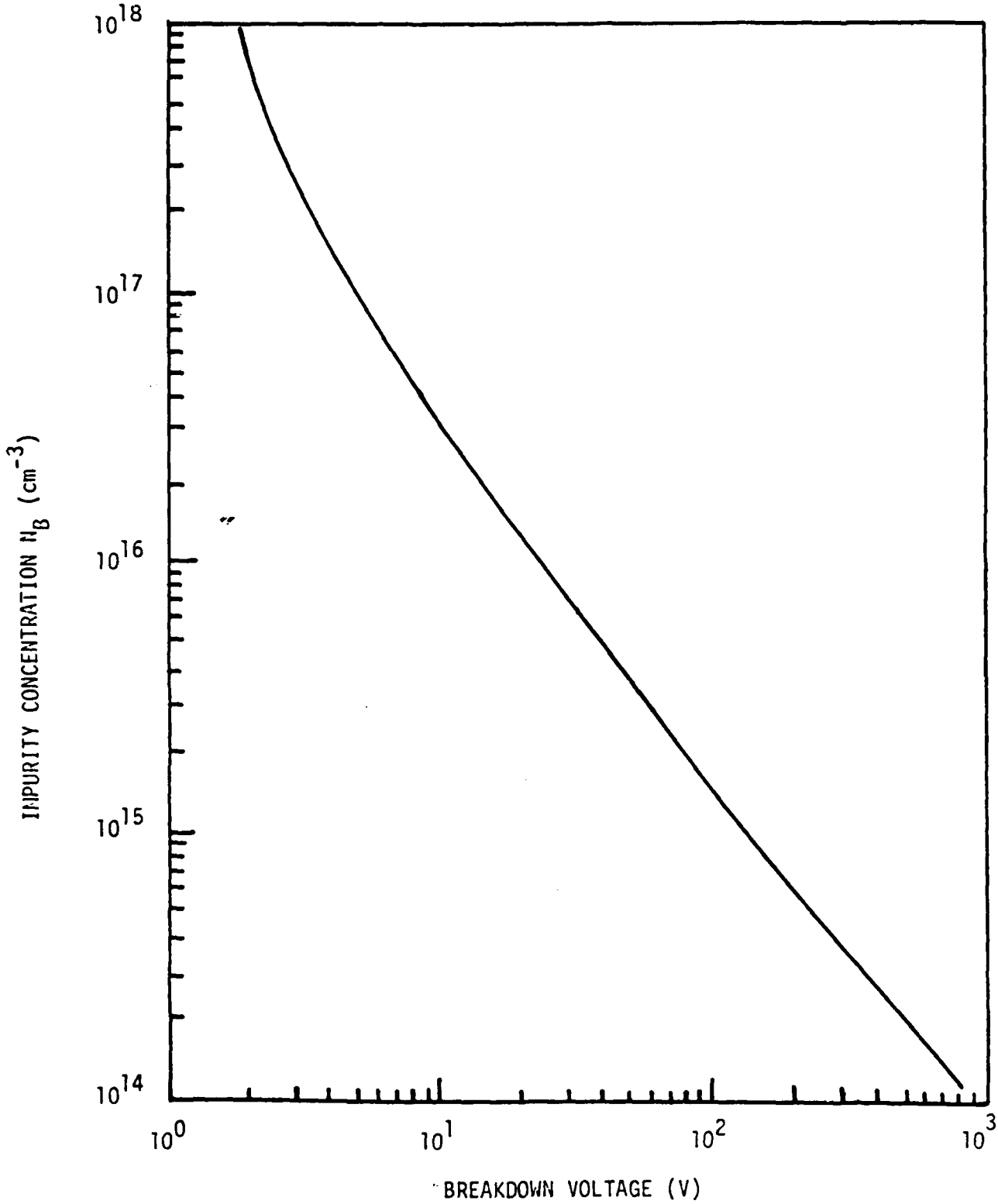

Fig. 3.3 Avalanche breakdown voltage vs impurity concentration for one-sided abrupt junction.

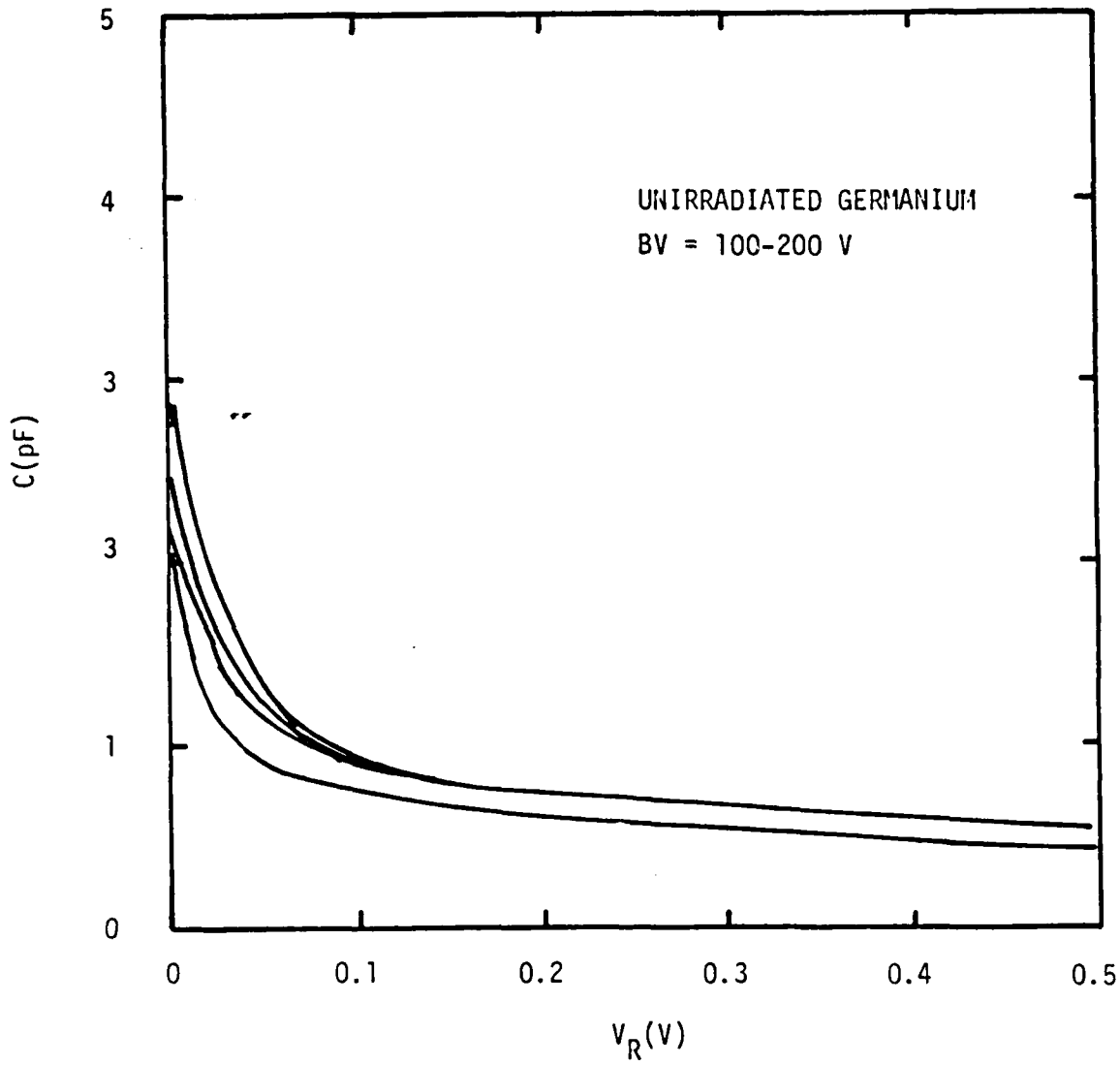

Fig. 3.4 Capacitance vs reverse-biased voltage for unirradiated Germanium of breakdown voltage between 100 and 200 V.

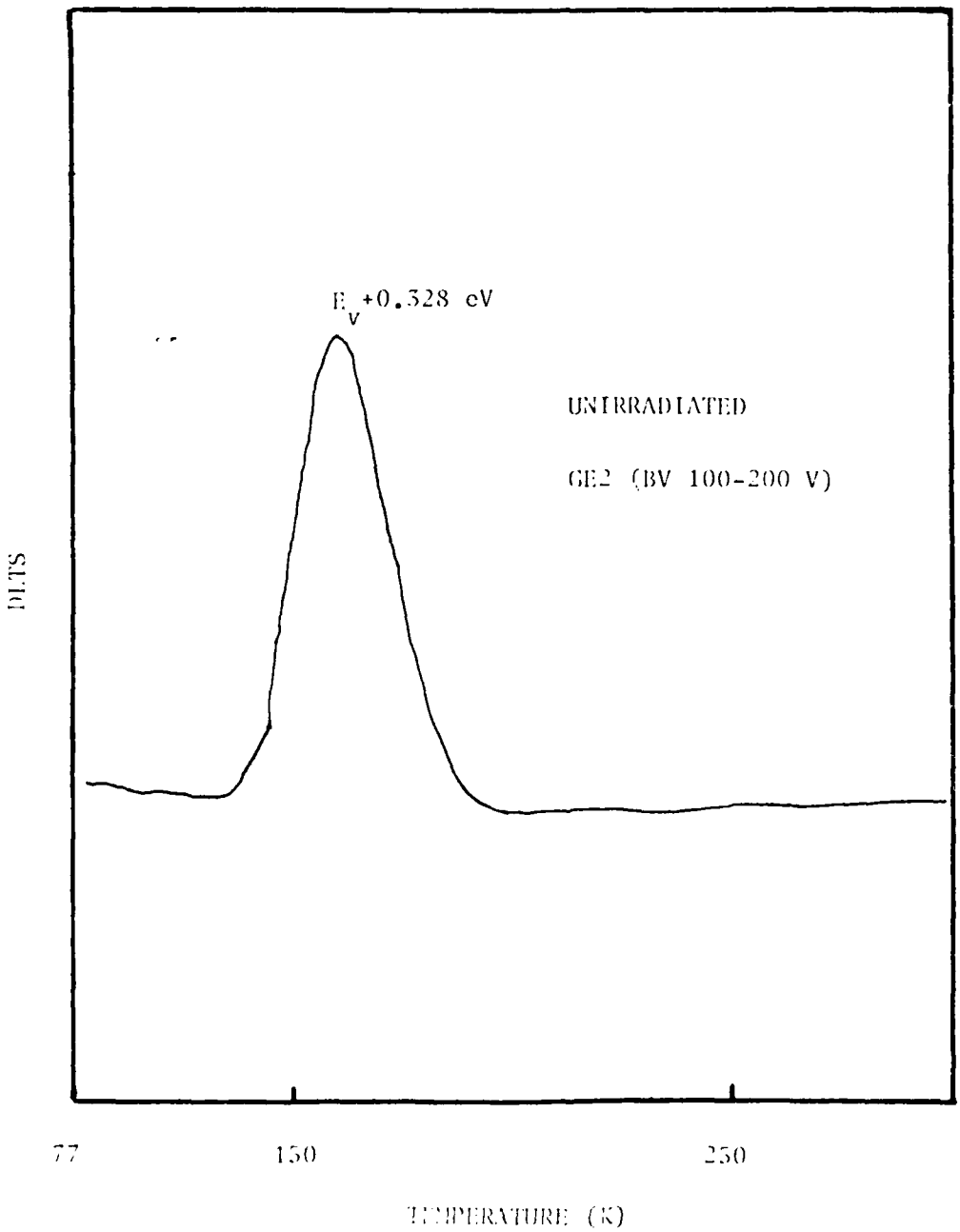

Fig. 3.15 DLTS scan of hole trap for unirradiated Germanium.

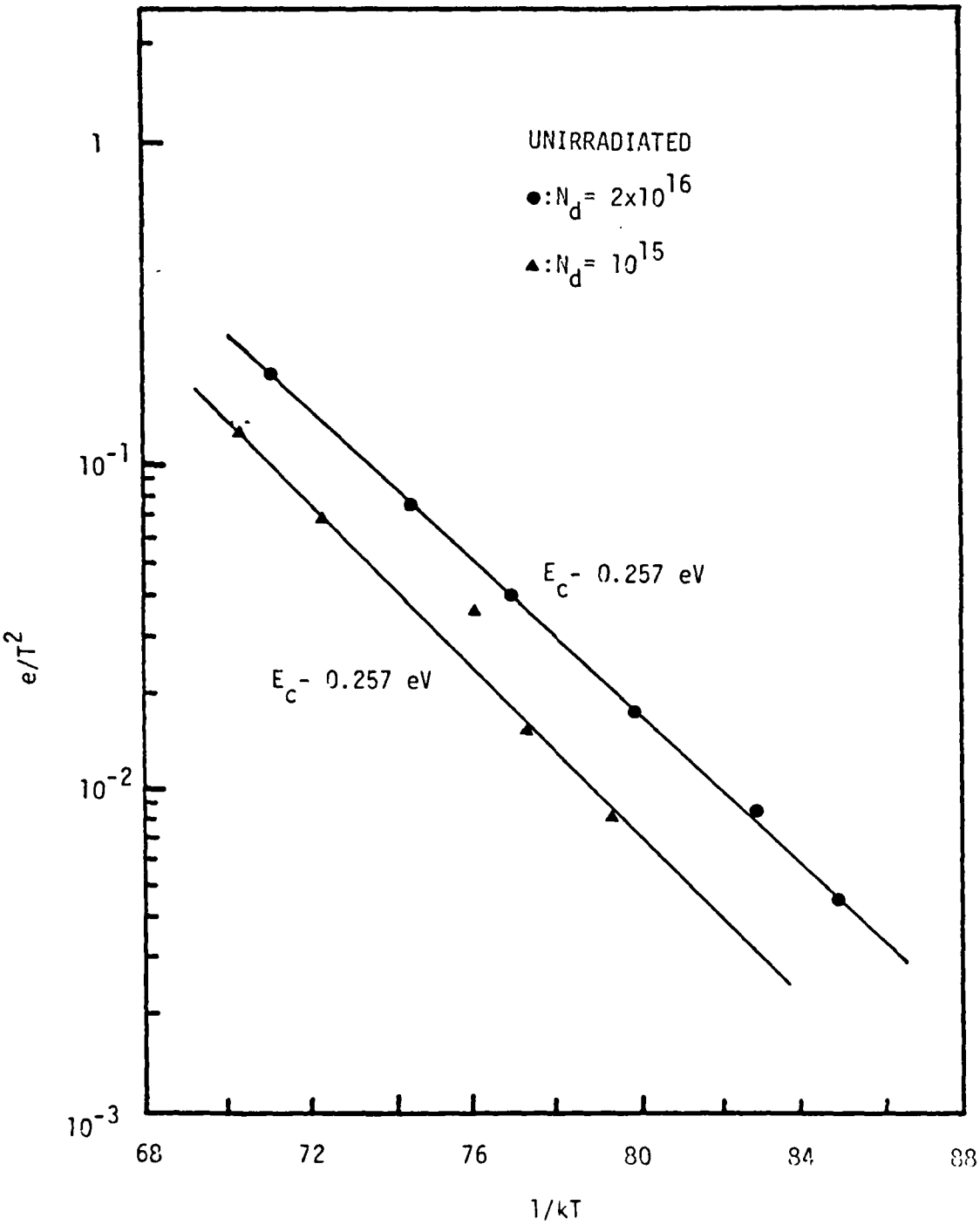

Fig. 3.14 The Arrhenius plot of defect level in unirradiated Germanium.

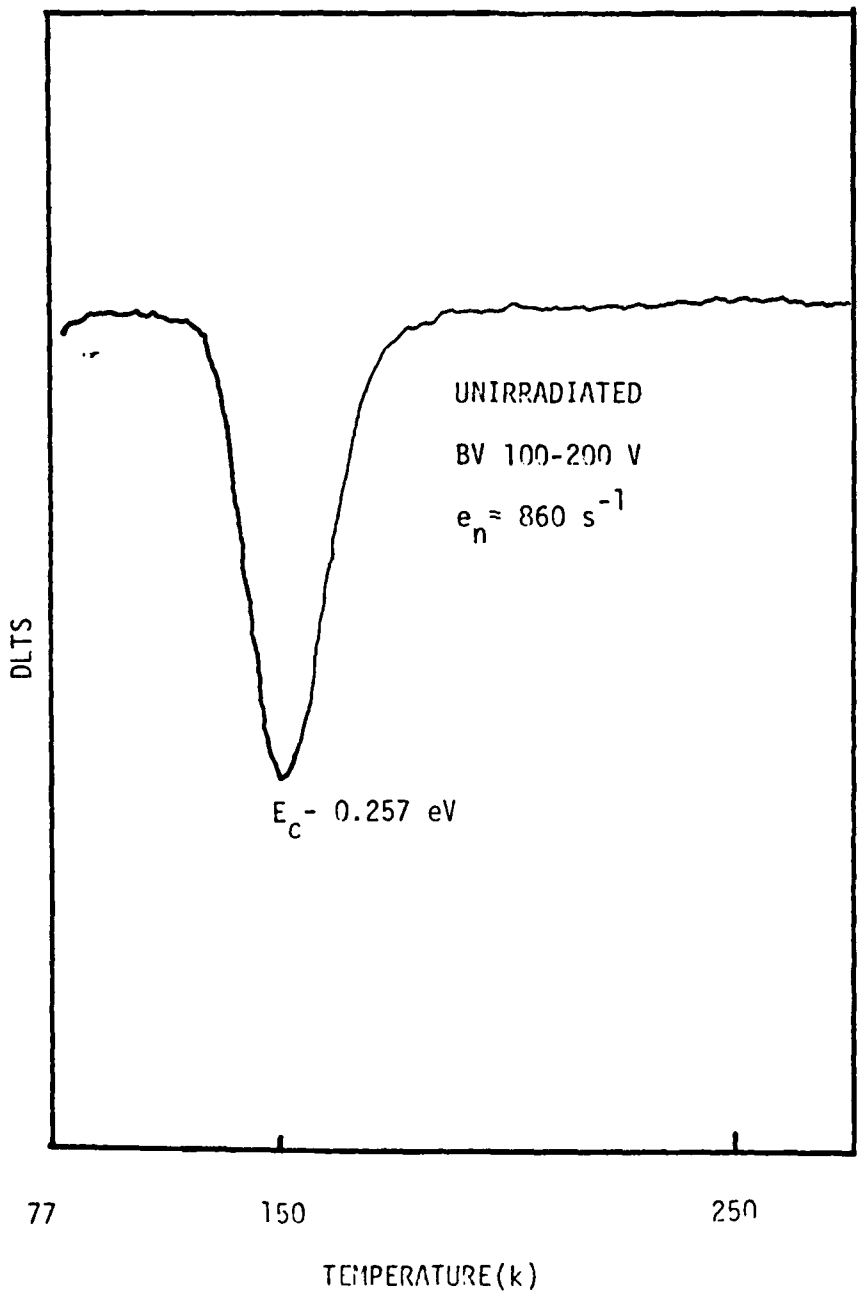

Fig. 3.13 DLTS scan of electron trap for unirradiated Germanium.

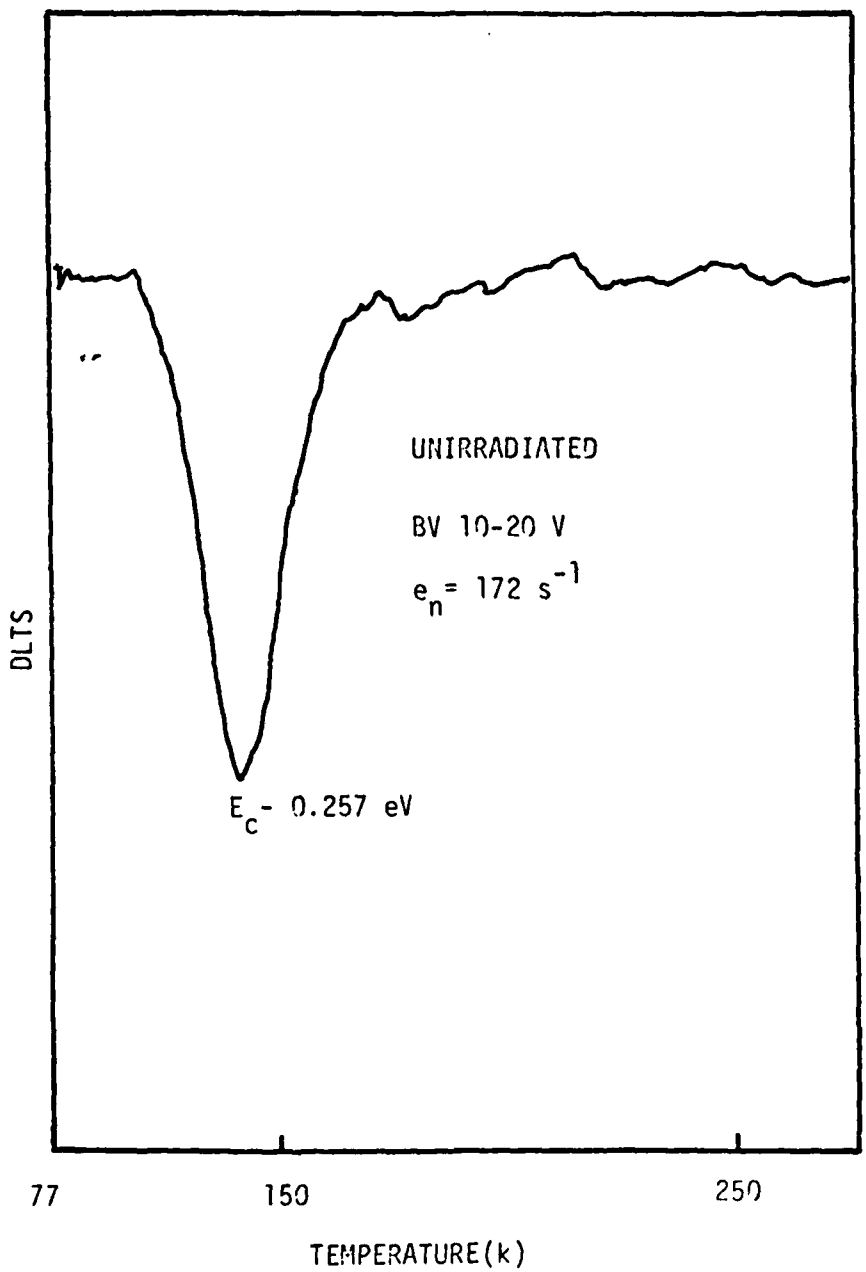

Fig. 3.12 DLTS scan of electron trap for Germanium irradiated by One-MeV electron.

Differentiating $S(\tau)$ with respect to τ and letting it equals to zero, yields

$$e_n^{-1} = \tau_{max} = (t_1-t_2)/\ln(t_1/t_2) \qquad (3.13)$$

which shows that $e_n = 1/\tau_{max}$ for each t_1 and t_2 setting. Thus, the time ratio t_1/t_2 can be fixed and the different setting of t_1 and t_2 produces several DLTS scans. The activation energy of the trap can be determined from the Arehnius plot of e_n/T^2 vs $1/kT$.

3.3.2 Results of the DLTS measurements

One-MeV electron irradiation with electron fluence, $\phi_e = 10^{14}$, 10^{15} and 10^{16} cm^{-2} are performed on germanium diodes with dopant density of $N_D = 10^{15}$ and $2x10^{16}$ cm^{-3}. These unirradiated germanium diodes contain copper imurity which has four levels (E_c- 0.26 eV, E_c+ 0.33 eV, E_v+ 0.04 and E_v+ 0.008 eV). Copper impurity is introduced regardless of the type doping material and methods of quenching [Reference 11]. From our DLTS measurements, the E_c- 0.26 eV and E_v+ 0.33 eV levels were observed in the unirradiated samples; these are shown in Fig.3. 12 to Fig.3. 16. However, it is likely that the substitutional copper impurity is moved to the interstitial site by the irradiation and finally precipitates to sinks like dislocations [Reference 6]. Hence, in the one-MeV electron irradiated germanium samples, the defect levels caused by the copper impuity is assumed not to be observed in the DLTS experiment. The very shallow levels caused directly or indirectly by copper impurity might exist [Reference 7]. The E_c- 0.27 eV level observed in diode with fluence of $\phi_e = 10^{15}$ cm^{-2}, which is very close to the E_c-0.26 eV due to the substitutional copper, is considered as the electron irradiation- induced defect. Fig. 3.9 shows the major defect levels reported in the literature. The dominant effect of bombardment of germanium is the introduction of acceptor type defects.

where $\Delta C = C_o - C(t)$, which is determined from the DLTS measurement. The junction capacitance and the background concentration N_D can be obtained from the C-V measurements. Thus, the defect concentration, N_t, can be calculated from Eq.(3.6).

The emission rate for an electron trap, which is functions of temperature, capture cross section and activation energy, can be written as

$$e_n = (\sigma_n \langle V_{th} \rangle N_c / g) \exp(-E_T/kT) \tag{3.7}$$

where σ_n is the electron capture cross section, $\langle v_{th} \rangle$ is the average thermal velocity of electrons; N_c is the effective conduction band states; g is the degeneracy factor, and E_T is the activation energy. Eq.(3.7) can be simplified to

$$e_n = BT^2 \exp(-E_T/kT) \tag{3.8}$$

where B is a proportionality constant which is independent of temperature. The capacitance transient is given by:

$$C(t) \cong C(o) \exp(-t/\tau) \tag{3.9}$$

where $\tau = e_n^{-1}$. The time setting t_1 and t_2 are determined by the dual gated boxcar averager, and the corresponding capacitance at t_1 and t_2 is given respectively by

$$C(t_1) = \Delta C \exp(-t_1/\tau) \tag{3.10}$$

$$C(t_2) = \Delta C \exp(-t_2/\tau) \tag{3.11}$$

The DLTS signal is obtained by taking the difference of Eq. (3.10) and (3.11) which yields

$$S(\tau) = \Delta C \left[\exp(-t_1/\tau) - \exp(-t_2/\tau)\right] \tag{3.12}$$

breakdown voltages. Plots of N_D versus $1/C^2$ are shown in Fig.3.6, 3.7, 3.11 and 3.12, respectively. For comparison, the calculated diode parameters are summarized in Table 3.1.

3.3.1 Theory of DLTS Technique

Deep-Level Transient Spectroscopy (DLTS) technique is a high frequency capacitance transient thermal scanning method which is useful for detecting a wide variety of traps including both radiative and non-radiative centers in semiconductors.

The DLTS technique reveals the spectrum of traps in a p/n junction or a Schottky diode, and from which one can measure the activation energy, defect concentration profile, and electron- and hole-capture cross sections for each trap level. The defect concentration is proportional to the peak height and this in turn is proportional to the capacitance change ΔC. Therefore, the defect concentration N_t is related to the capacitance change, ΔC, by the relation:

$$C(t) = [q\epsilon_s(N_D-N_t)/2(V_{bi}+V_R)]^{1/2}$$

$$= C_o(1-N_t/N_D)^{1/2} \qquad (3.4)$$

where $C_o = C(V_R) = [q\epsilon_s N_D/2(V_{bi}+V_R)]^{1/2}$ is the junction capacitance at the quiescent reverse bias; V_{bi} is the built-in potential. Using the binomial expansion and the condition that $N_t/N_D \ll 1$, Eq. (3.4) reduces to a simpler form as:

$$C(t) \cong C_o(1 - N_t(t)/2N_D) \qquad (3.5)$$

Thus, the trap density os related to the change in capacitance by:

$$N_t = (2\Delta C/C_o)N_D \qquad (3.6)$$

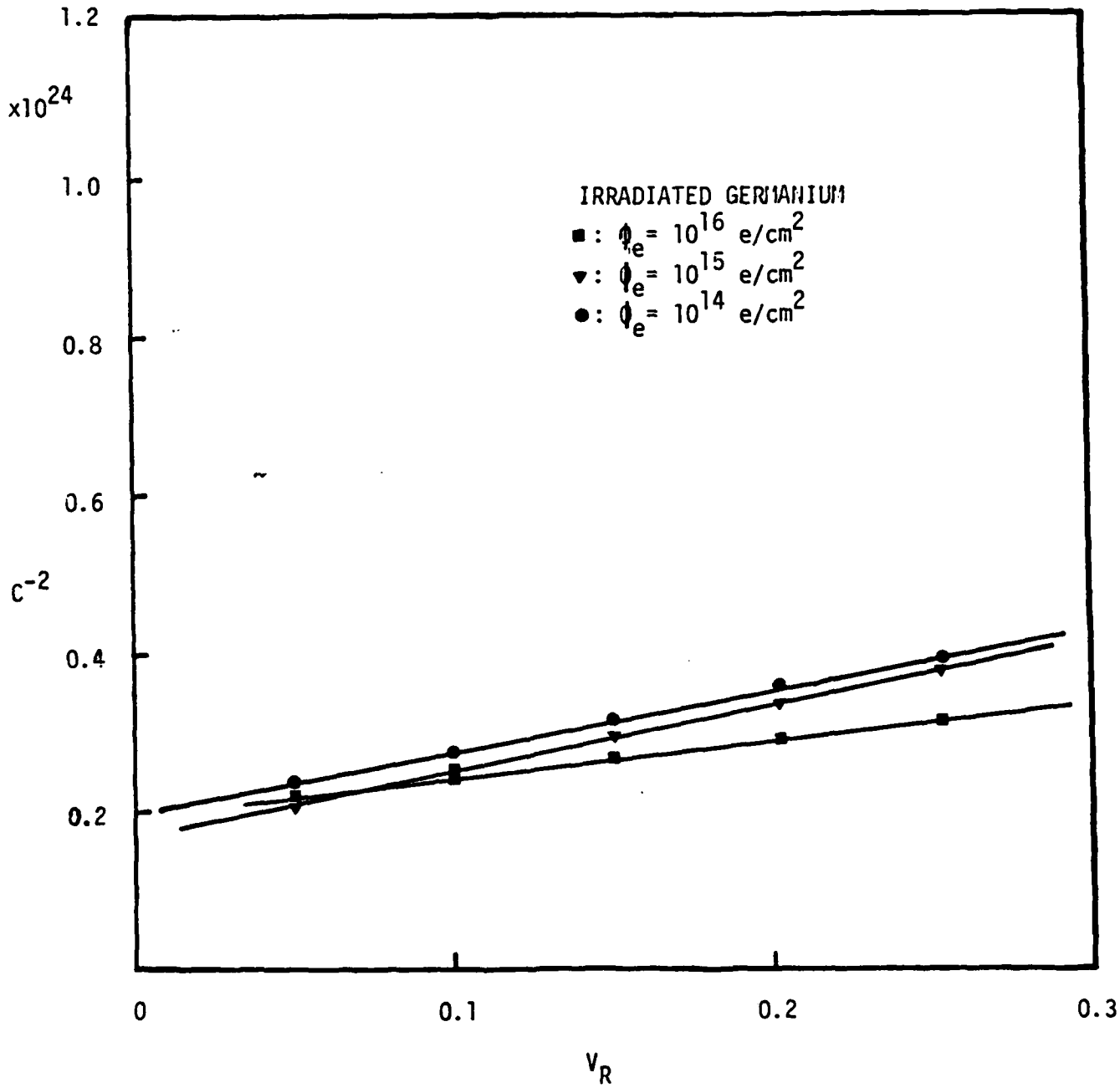

Fig. 3.11 C^{-2} vs reverse-biased voltage for Germanium of breakdown voltage between 10 and 20 V irradiated by One-MeV electron.

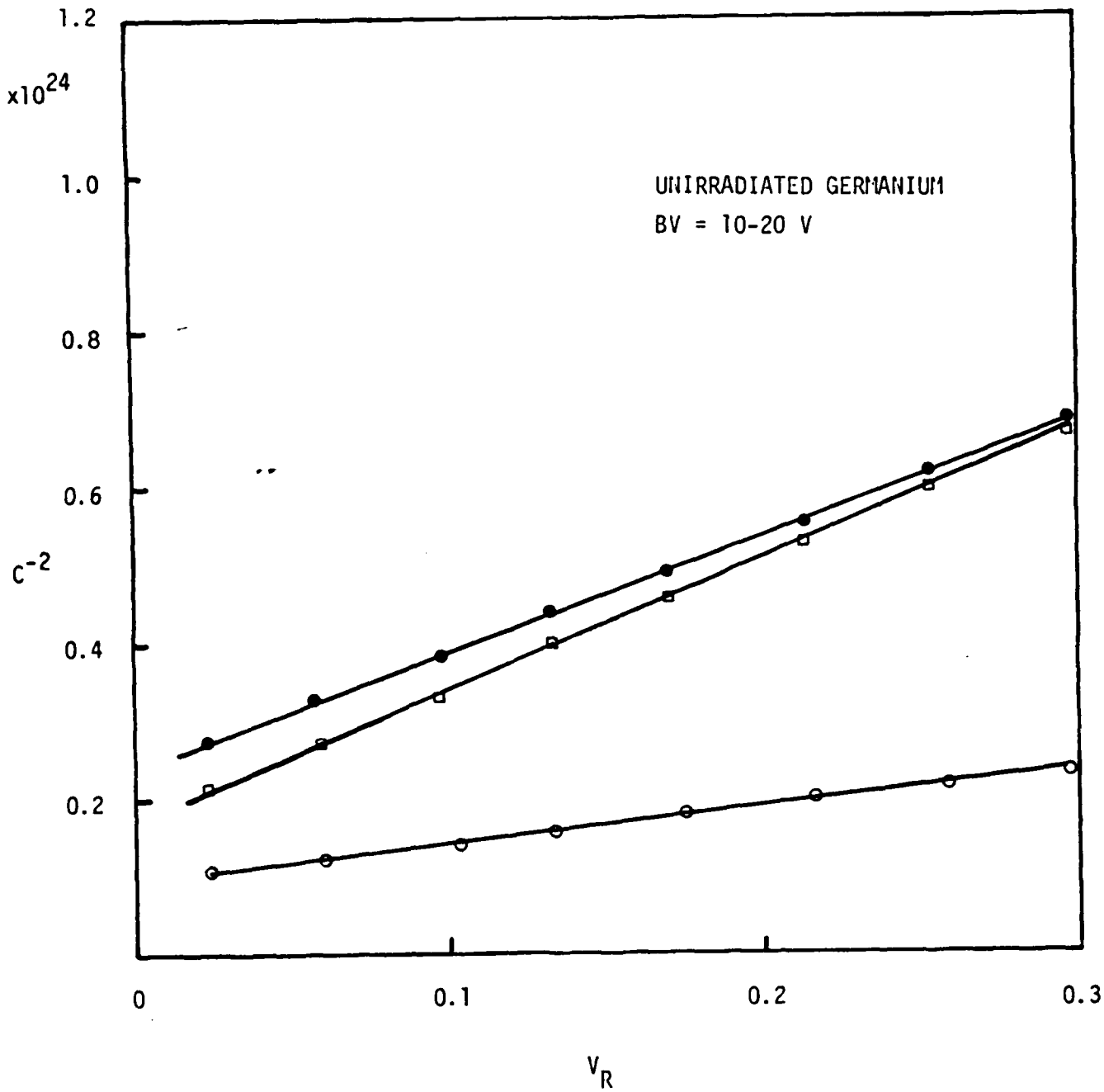

Fig. 3.10 C^{-2} vs reverse-biased voltage for unirradiated Germanium of breakdown voltage between 10 and 20 V.

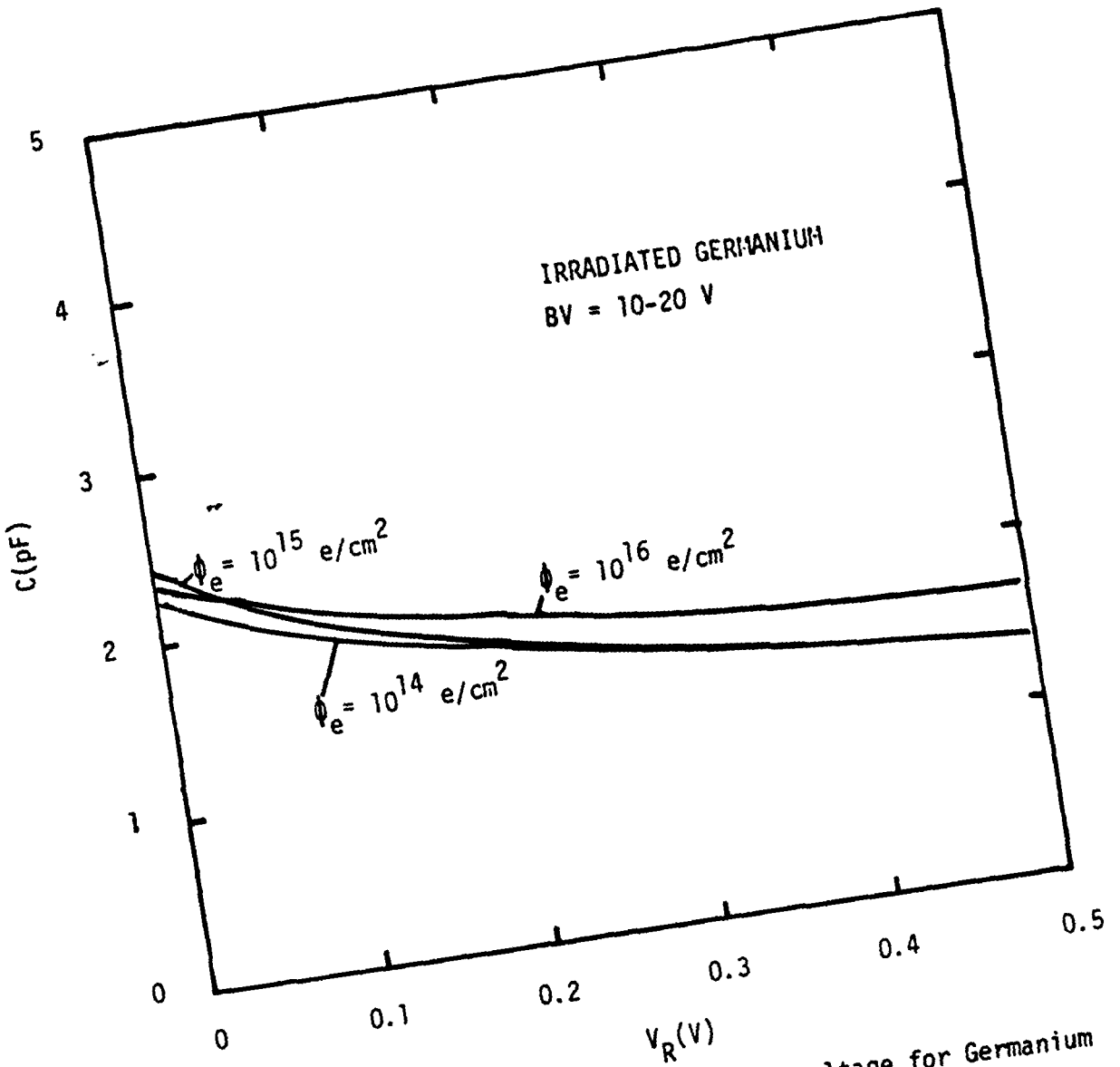

Fig. 3.9 Capacitance vs reverse-biased voltage for Germanium of breakdown voltage between 10 and 20 V irradiated by One-MeV electron.

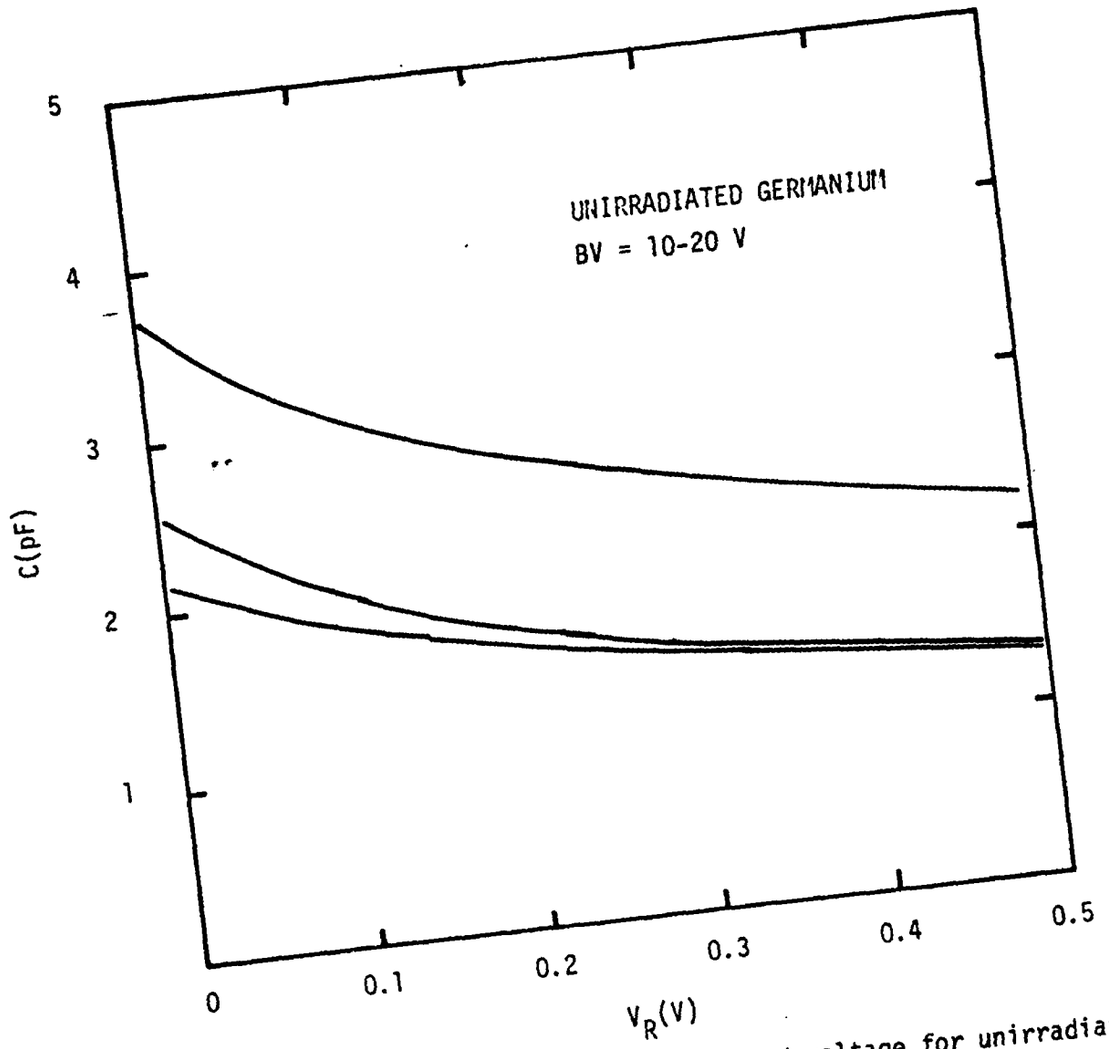

Fig. 3.8 Capacitance vs reverse-biased voltage for unirradiated Germanium of breakdown voltage between 10 and 20 V.

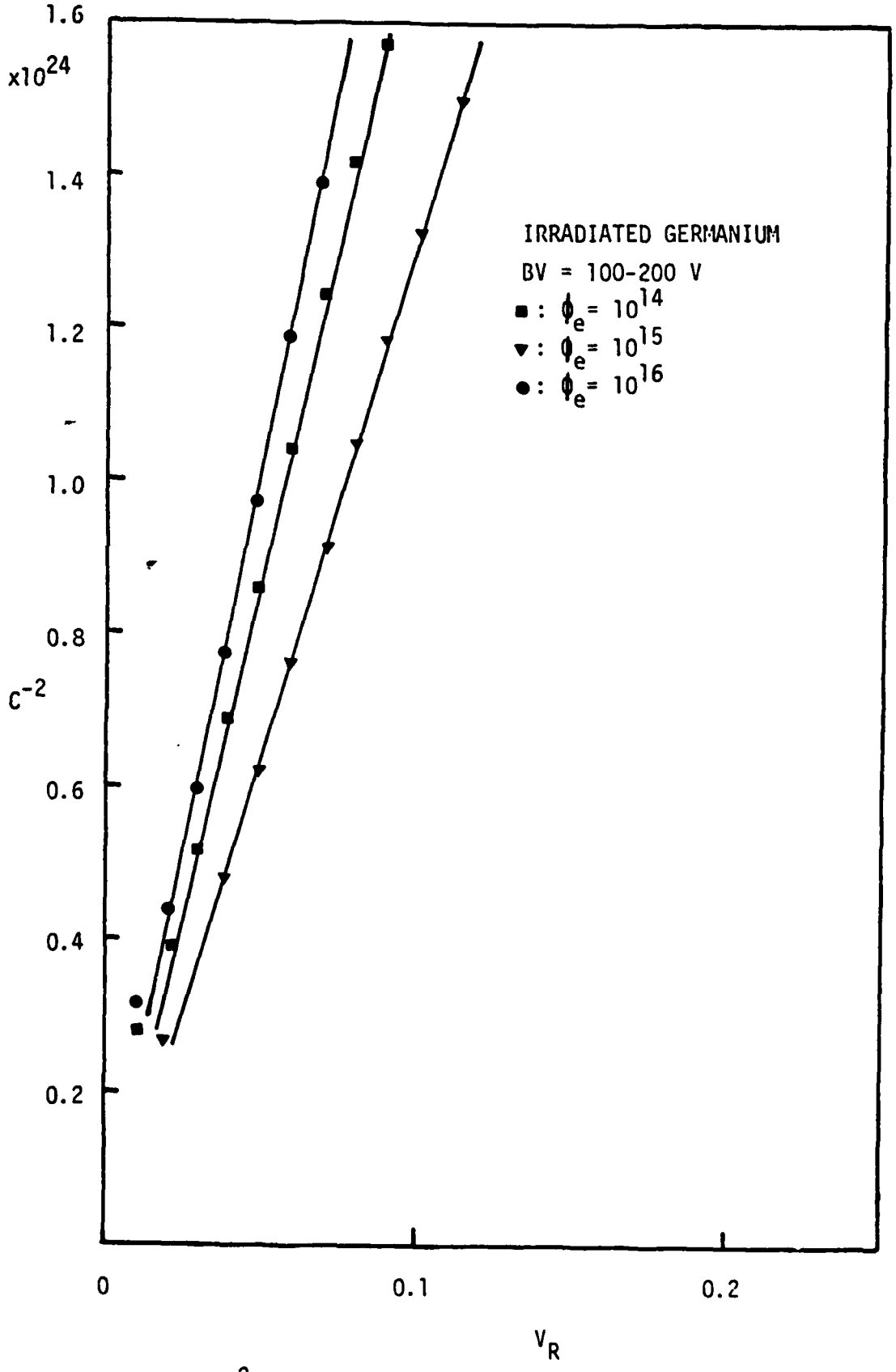

Fig. 3.7 C^{-2} vs reverse-biased voltage for Germanium of breakdown voltage between 100 and 200 V irradiated by One-MeV electron.

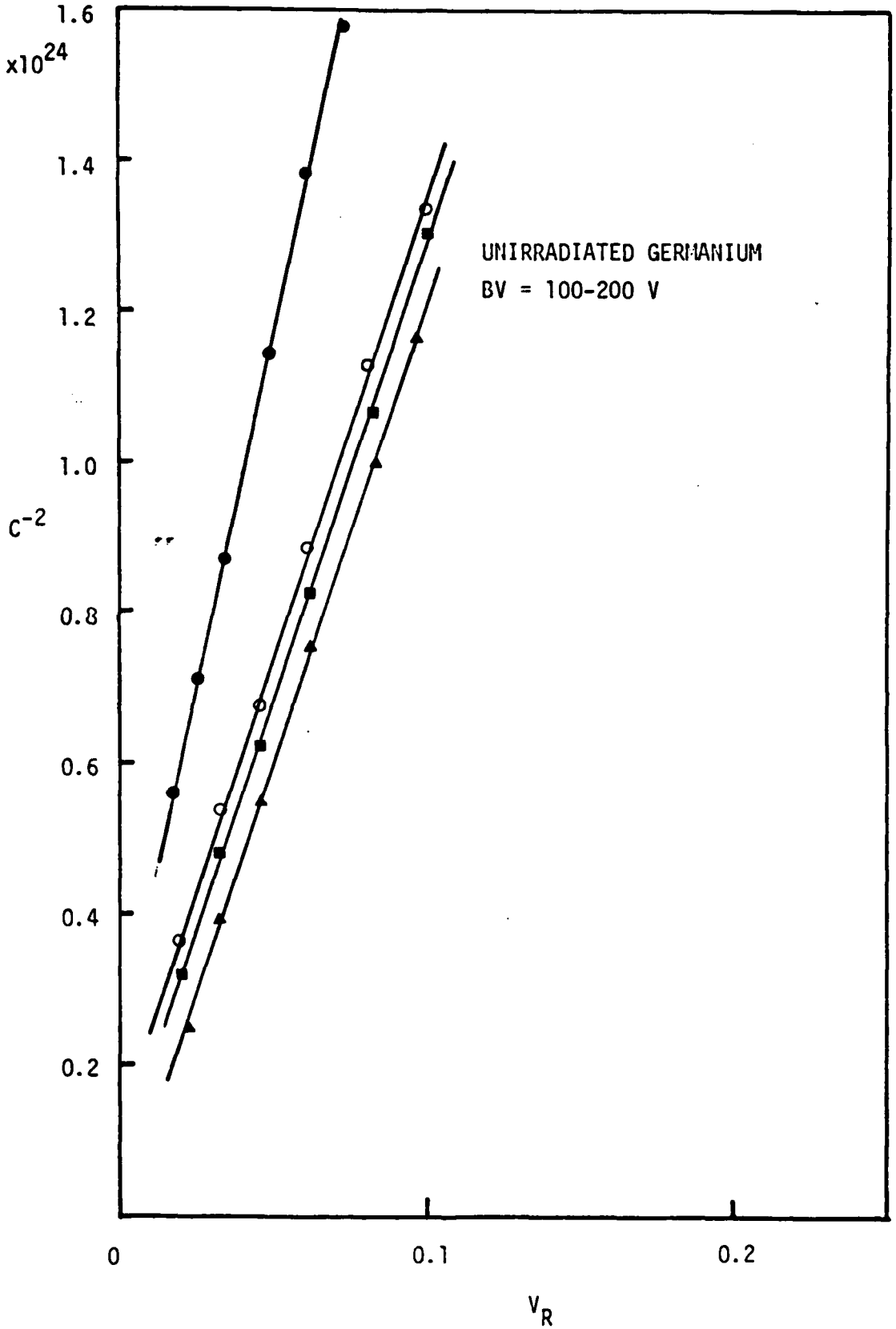

Fig. 3.6 C^{-2} vs reverse-biased voltage for unirradiated Germanium of breakdown voltage between 100 and 200 V.

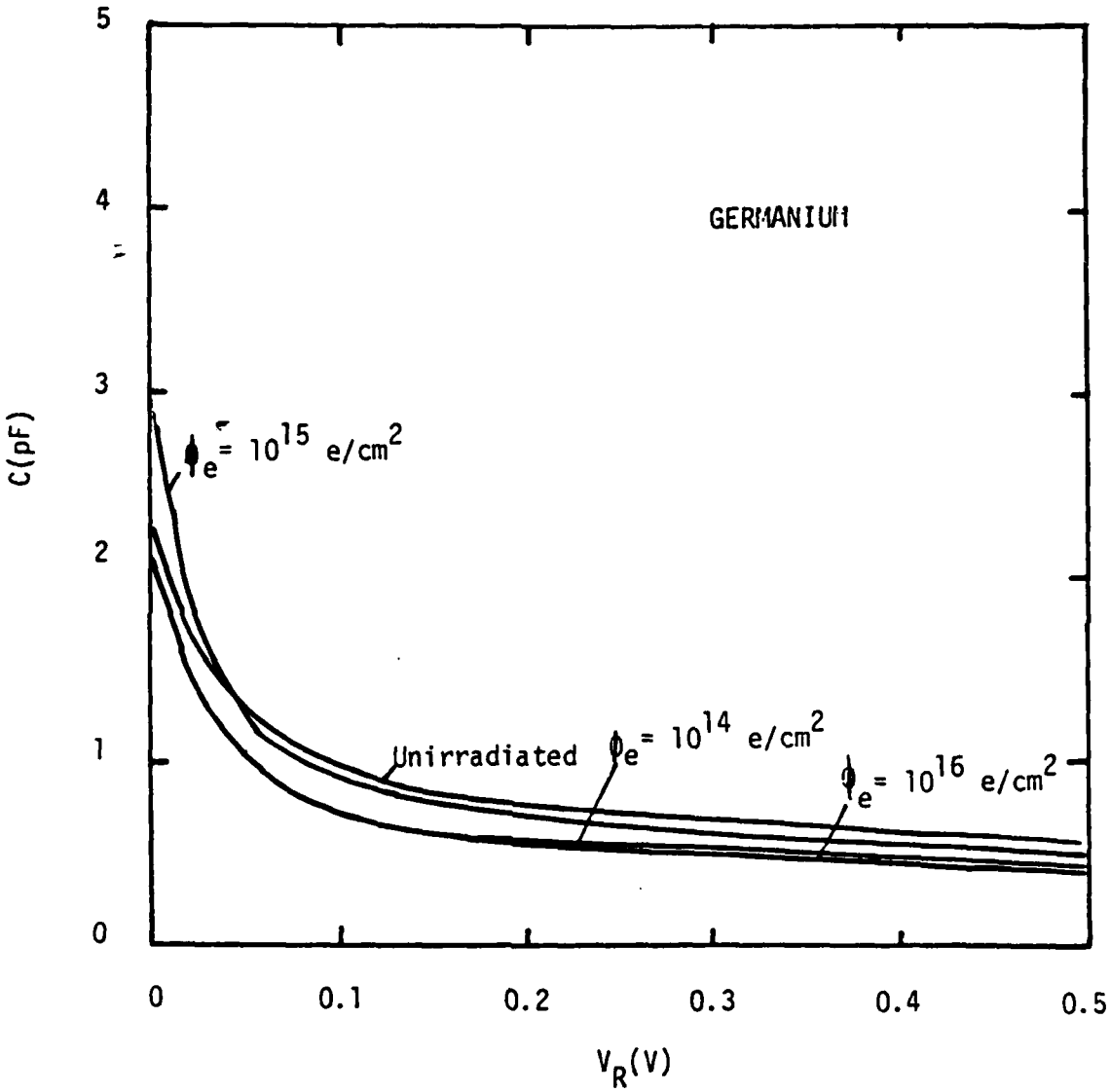

Fig. 3.5 Capacitance vs reverse-biased voltage for Germanium irradiated by One-MeV electron with breakdown voltage between 100 and 200 V.

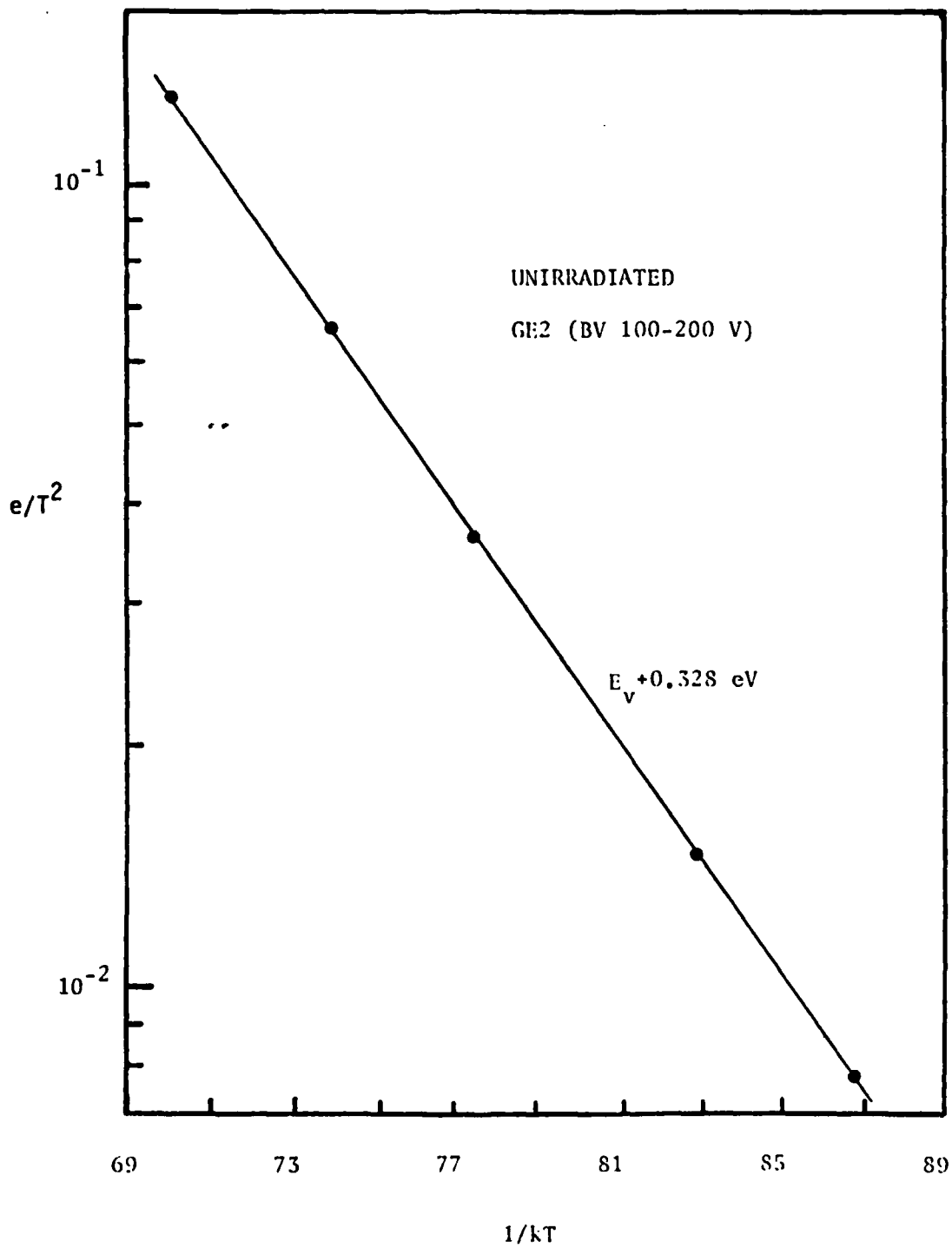

Fig. 3.16 Arrhenius plot of hole trap for unirradiated Germanium.

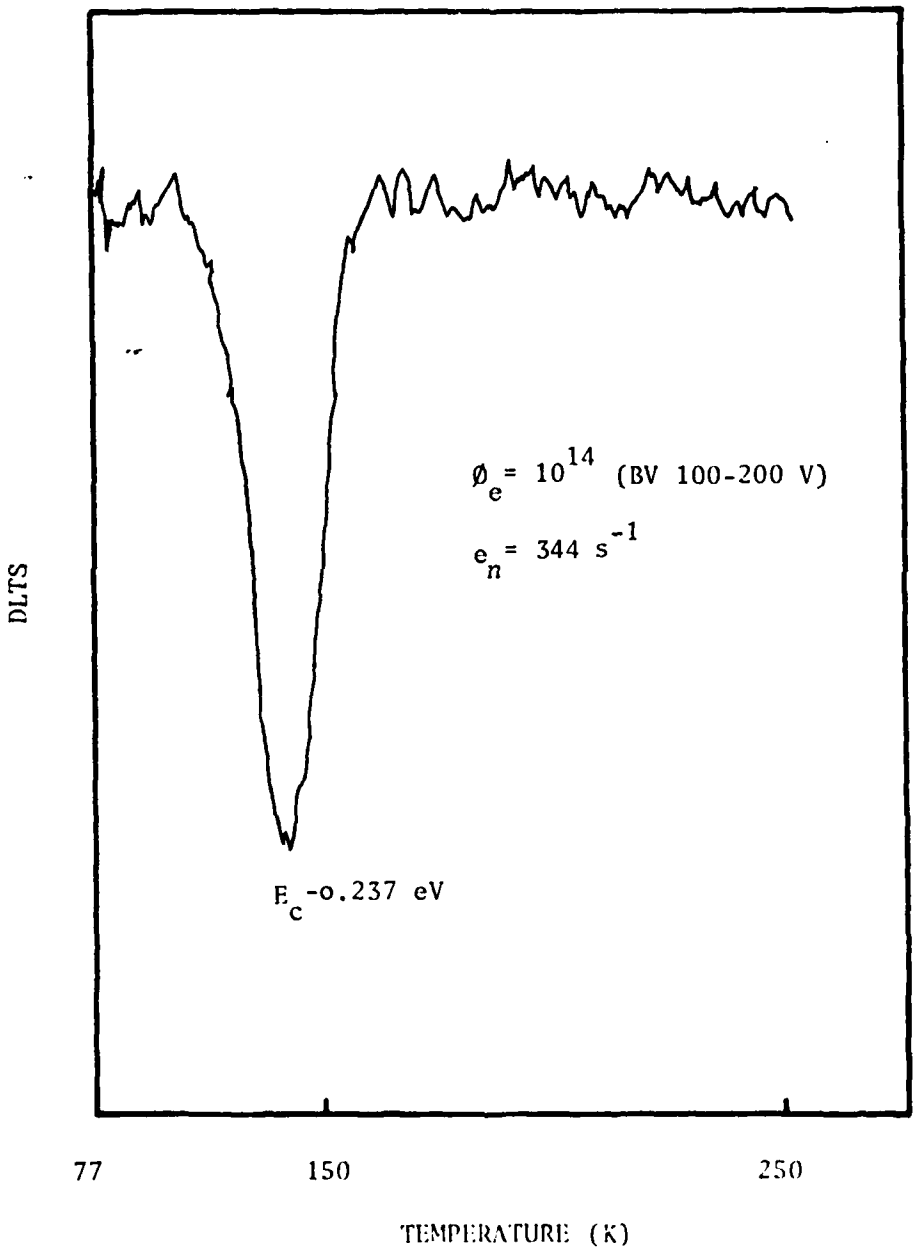

Fig. 3.17 DLTS scan of electron trap for Germanium irradiated by One-MeV electron.

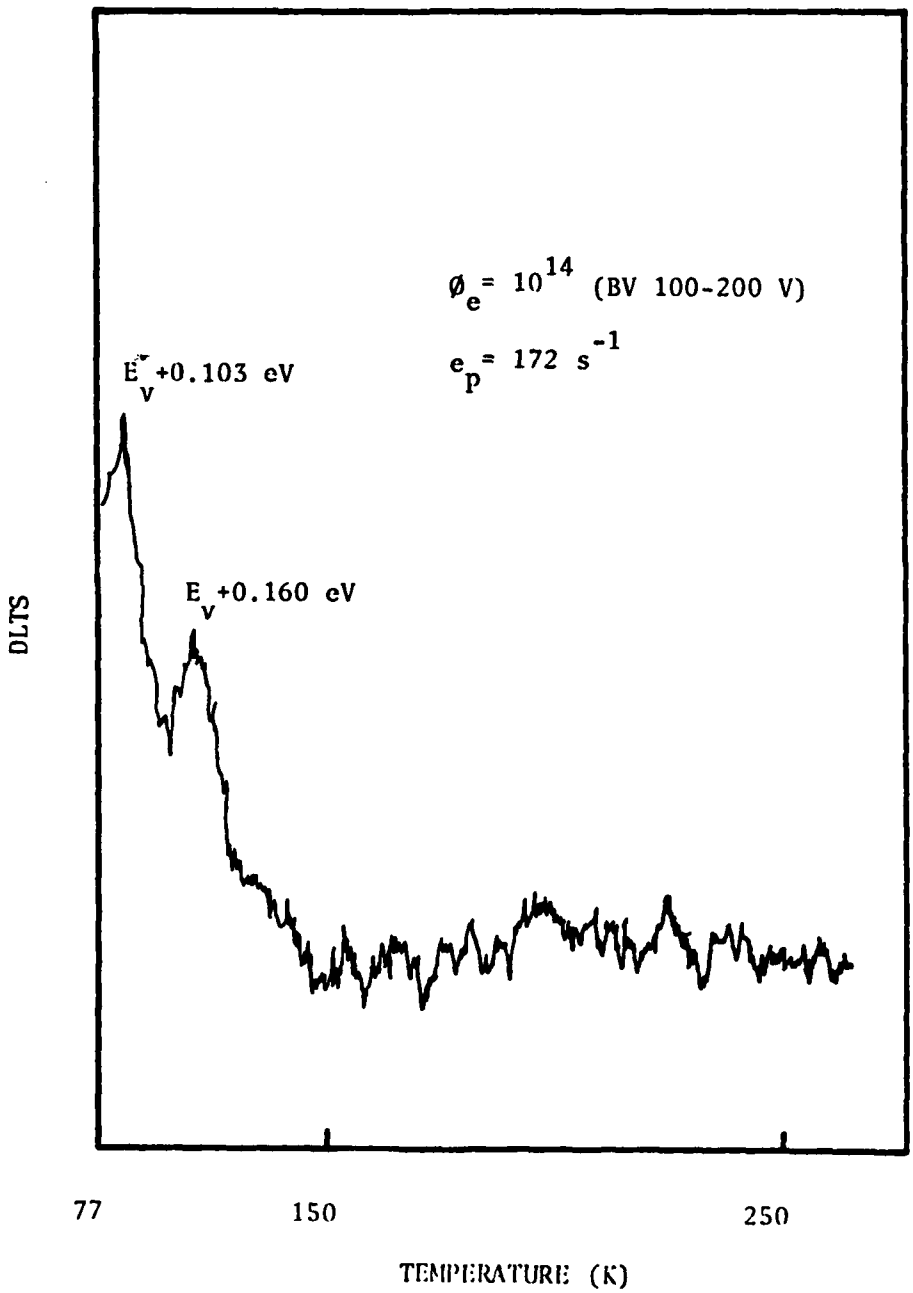

Fig. 3.18 DLTS scan of hole trap for Germanium irradiated by One-MeV electron.

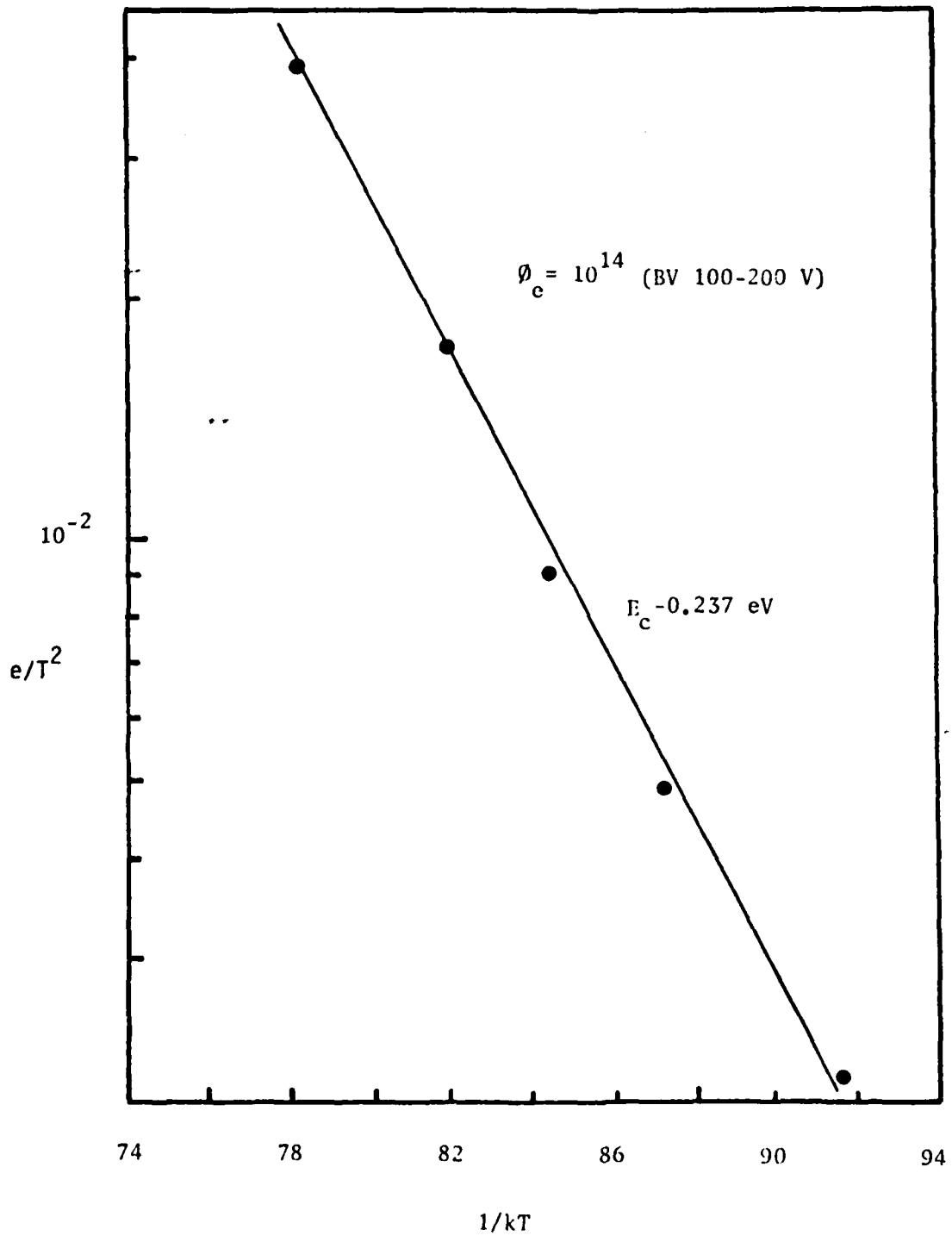

Fig. 3.19 Arrhenius plot of electron trap for Germanium irradiated by One-MeV electron.

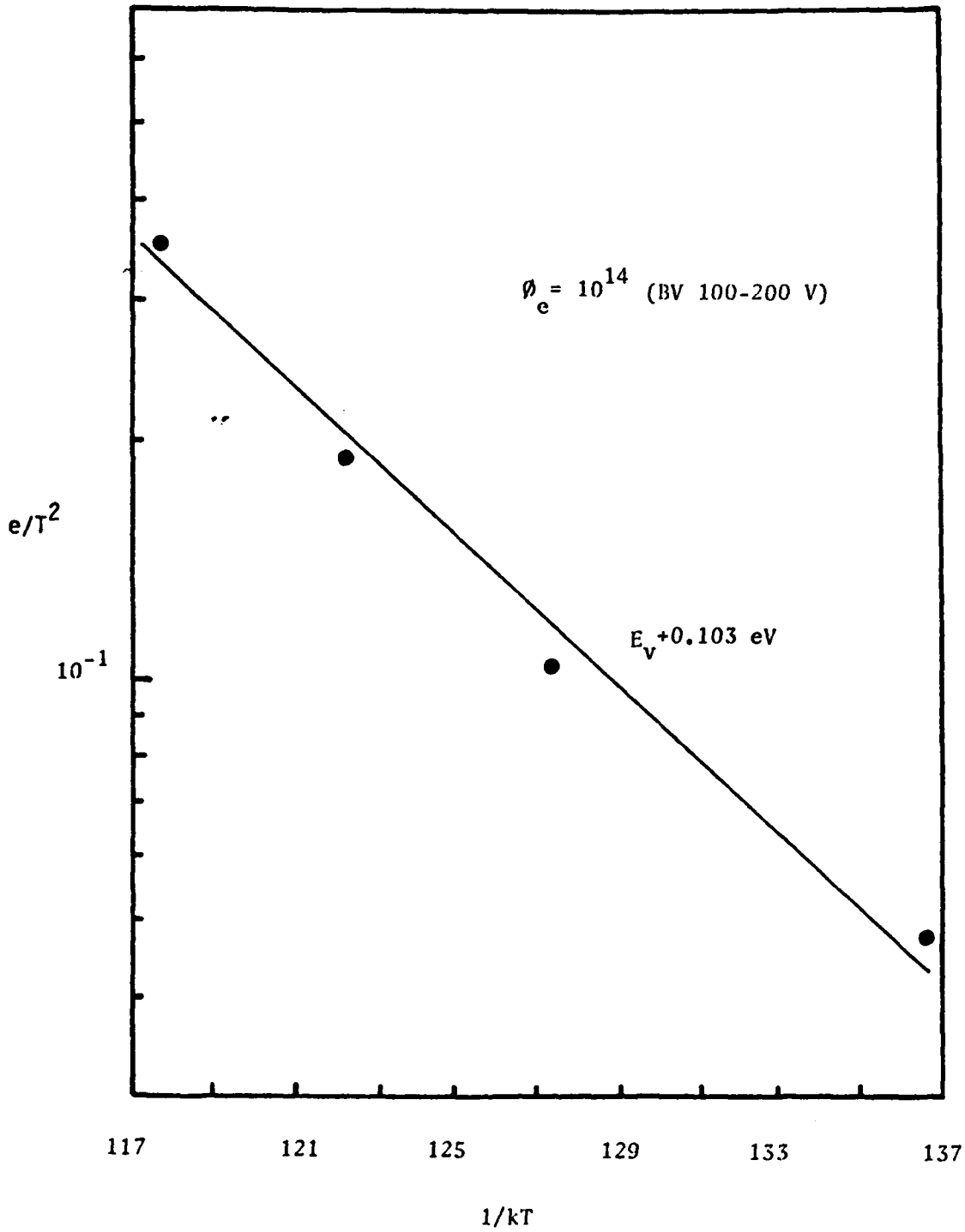

Fig. 3.20 Arrhenius plot of hole trap for Germanium irradiated by One-MeV electron.

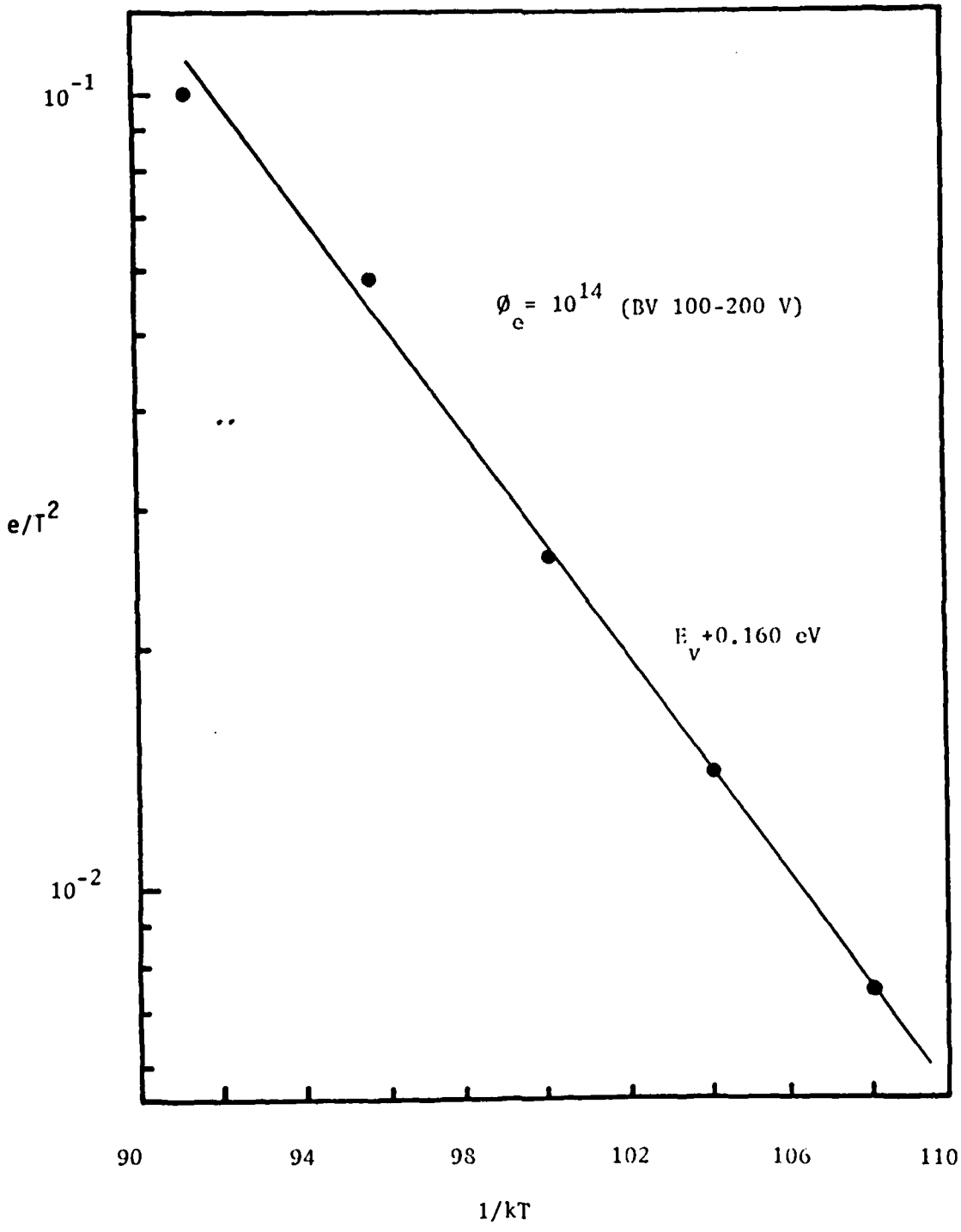

Fig. 3.21 Arrhenius plot of hole trap for Germanium irradiated by One-MeV electron.

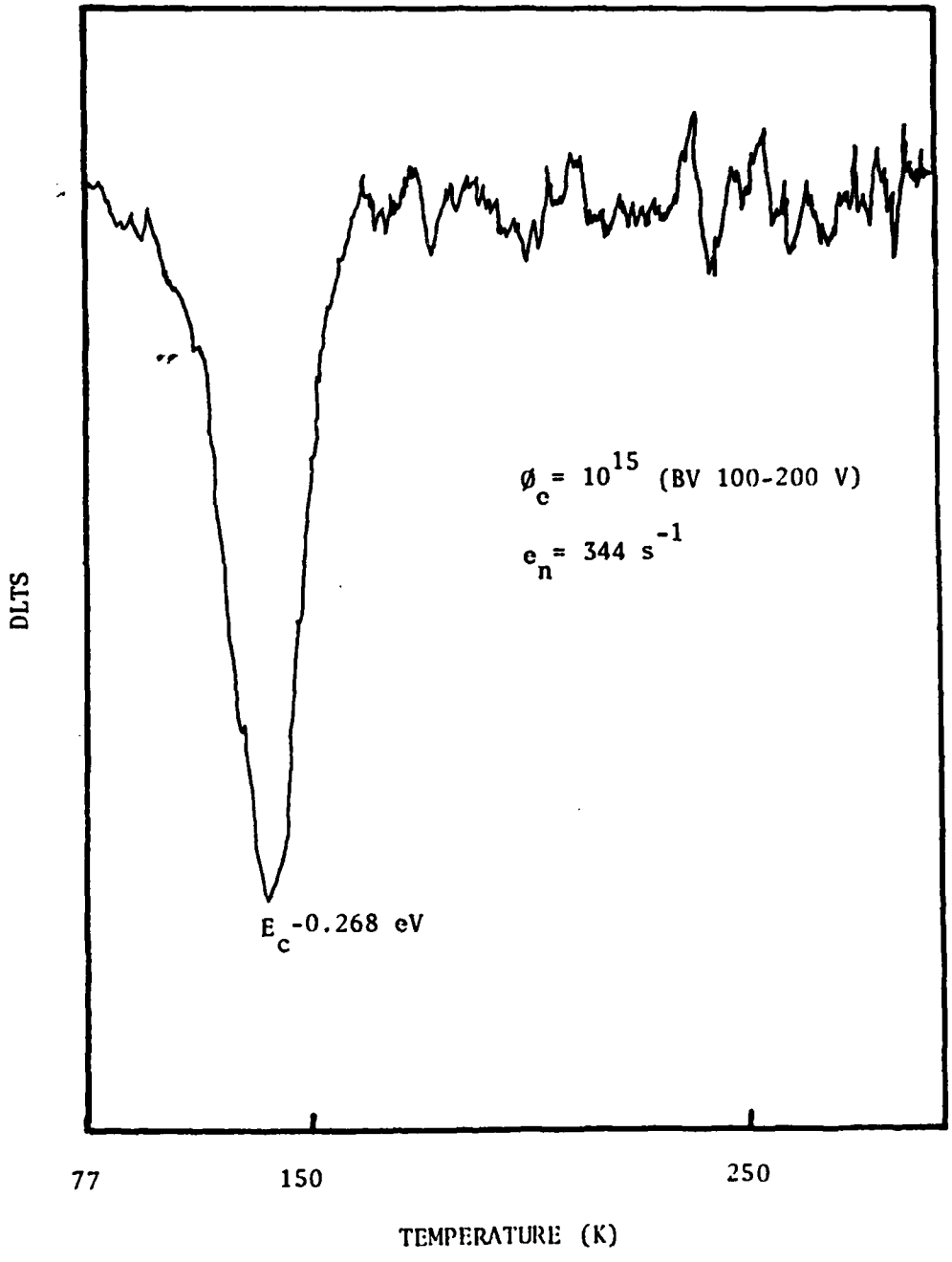

Fig. 3.22 The DLTS scan of electron trap for Germanium irradiated by One-MeV electron.

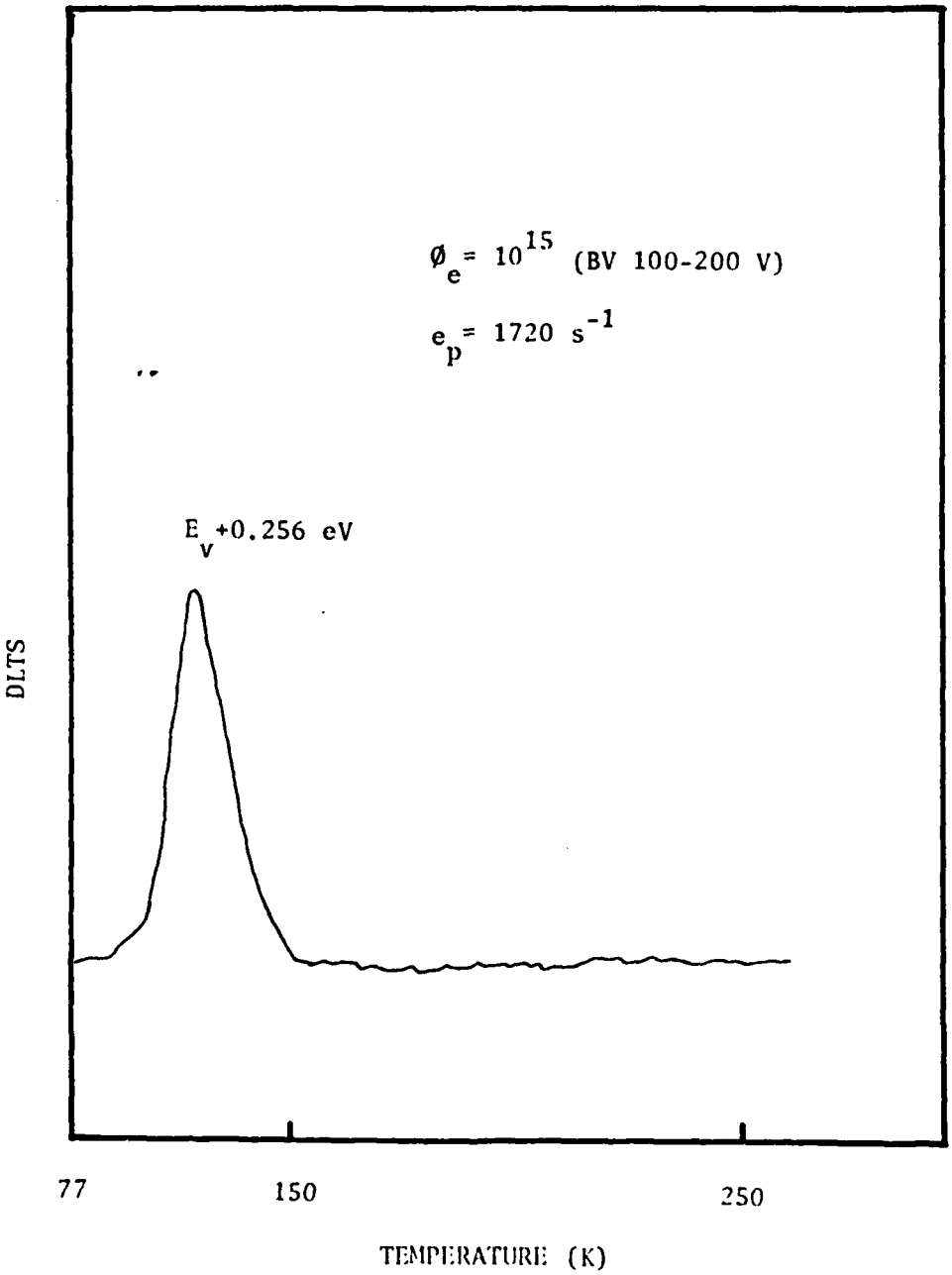

Fig. 3.23 The DLTS scan of hole trap for Germanium irradiated by One-MeV electron.

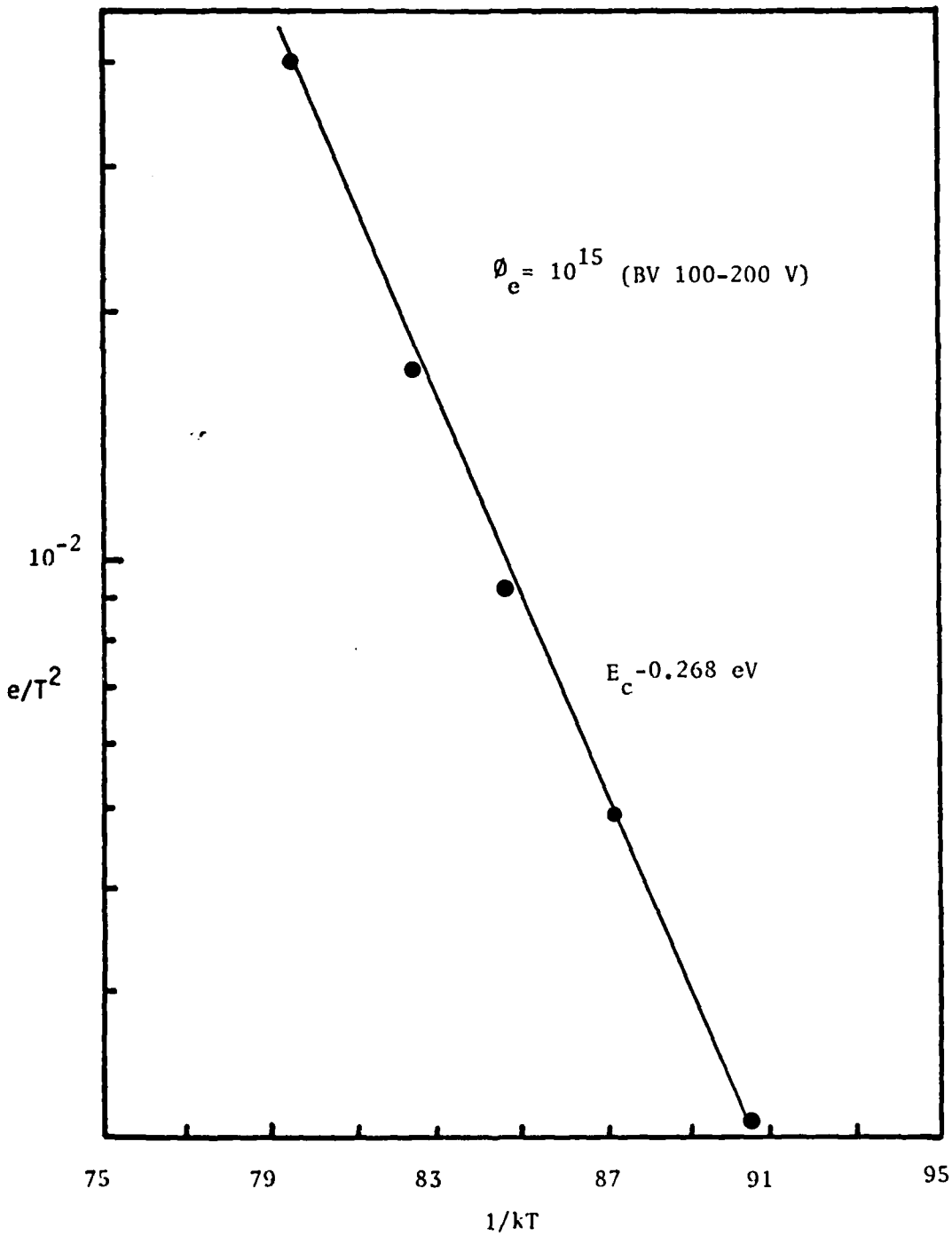

Fig. 3.24 Arrhenius plot of electron trap for Germanium irradiated by One-MeV electron.

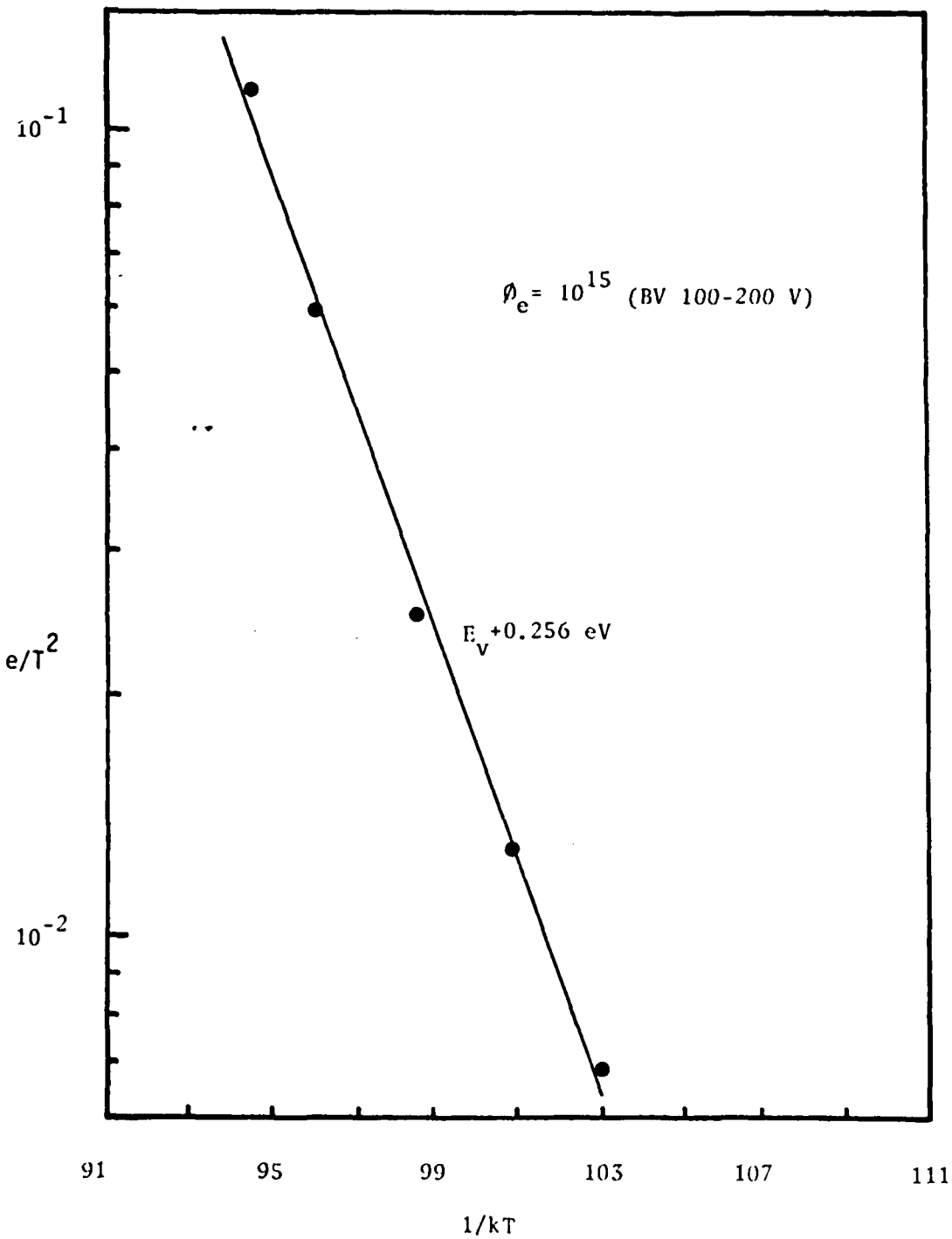

Fig. 3.25 Arrhenius plot of hole trap for Germanium irradiated by One-MeV electron.

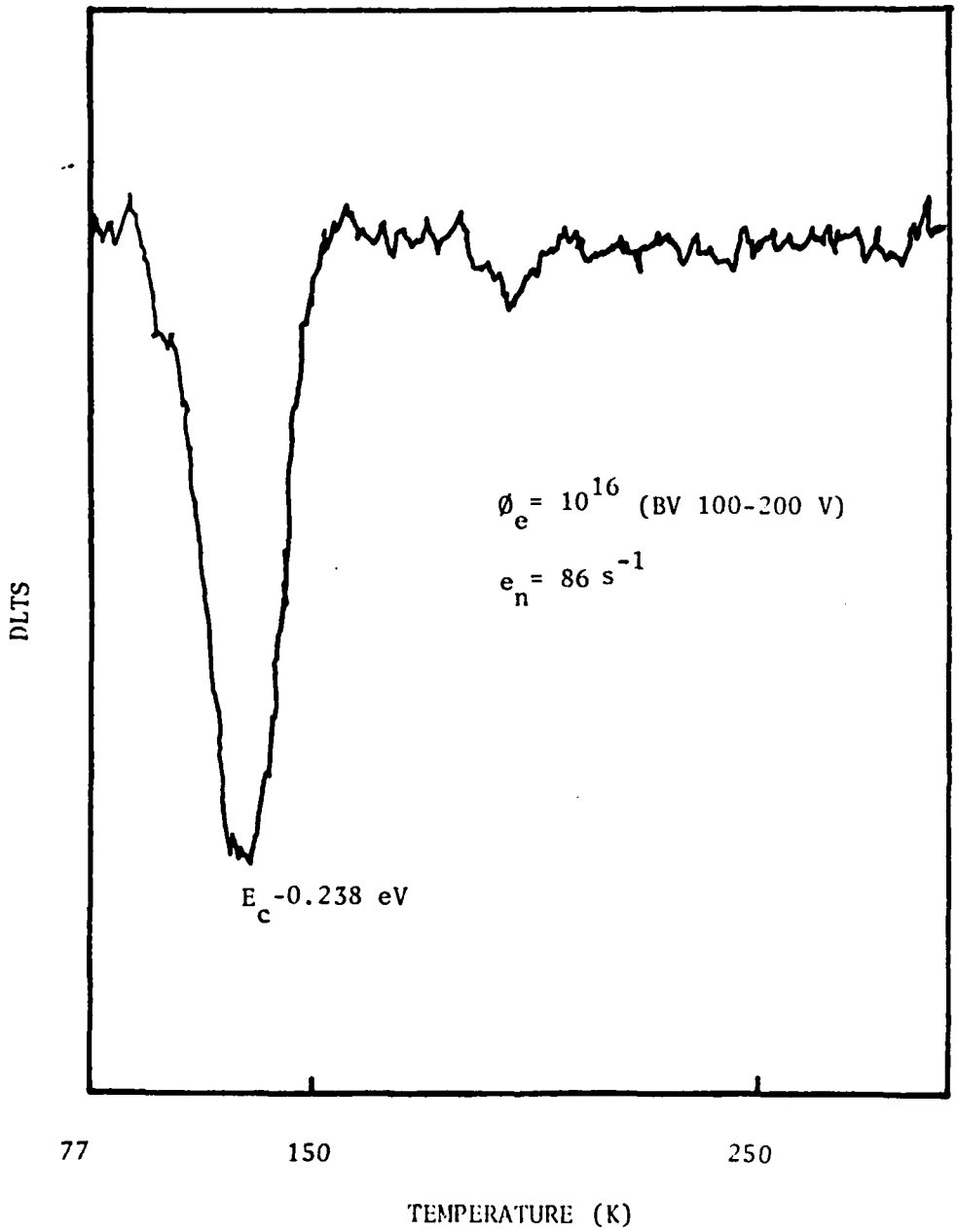

Fig. 3.26 DLTS scan of electron trap for Germanium irradiated by One-MeV electron.

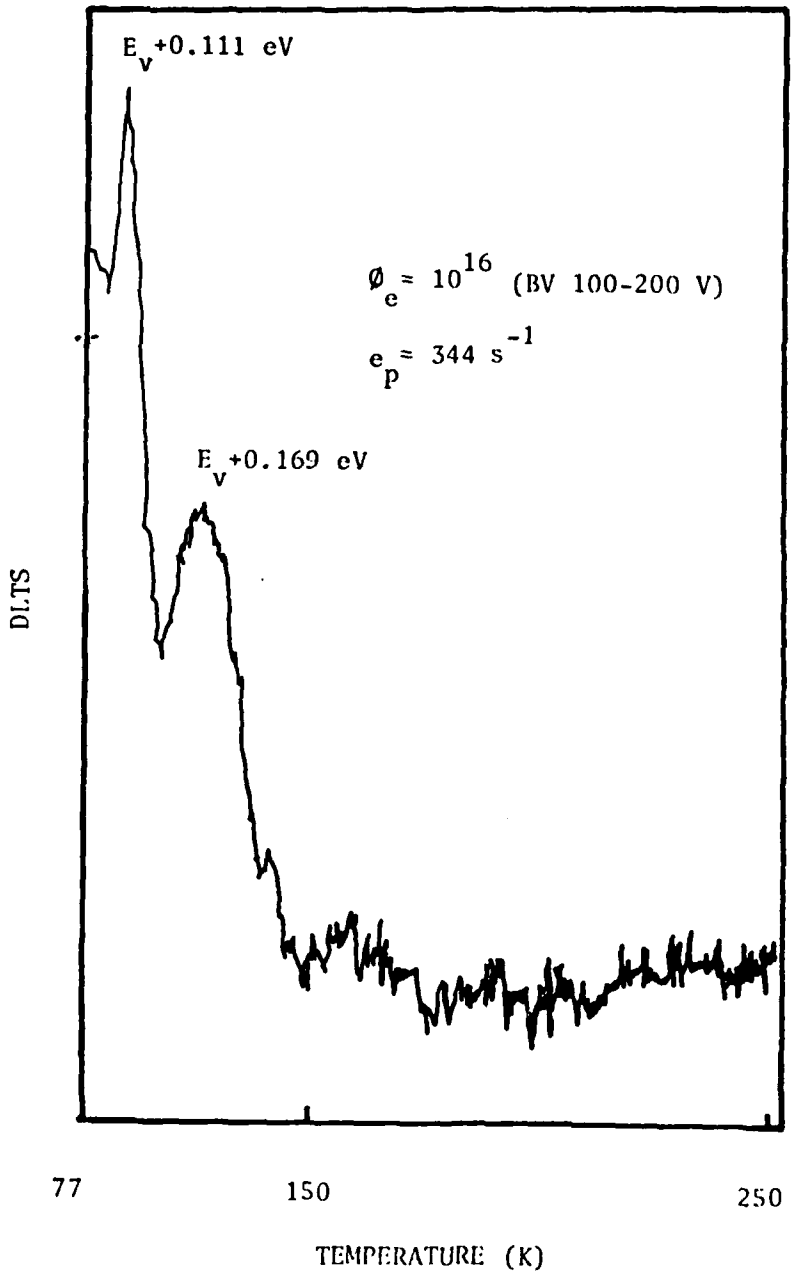

Fig. 3.27 DLTS scan of hole trap for Germanium irradiated by One-MeV electron.

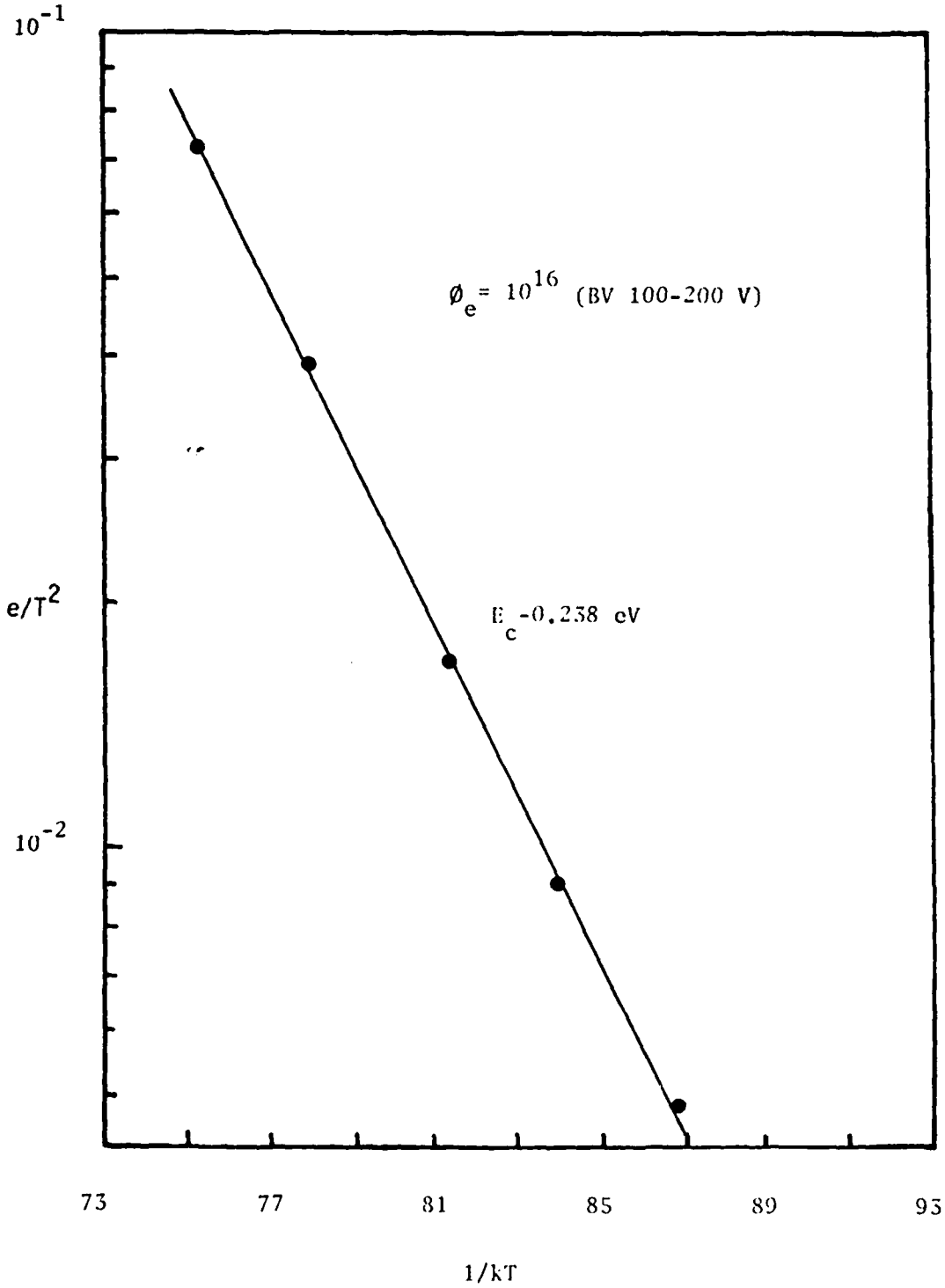

Fig. 3.28 Arrhenius plot of electron trap for Germanium irradiated by One-MeV electron.

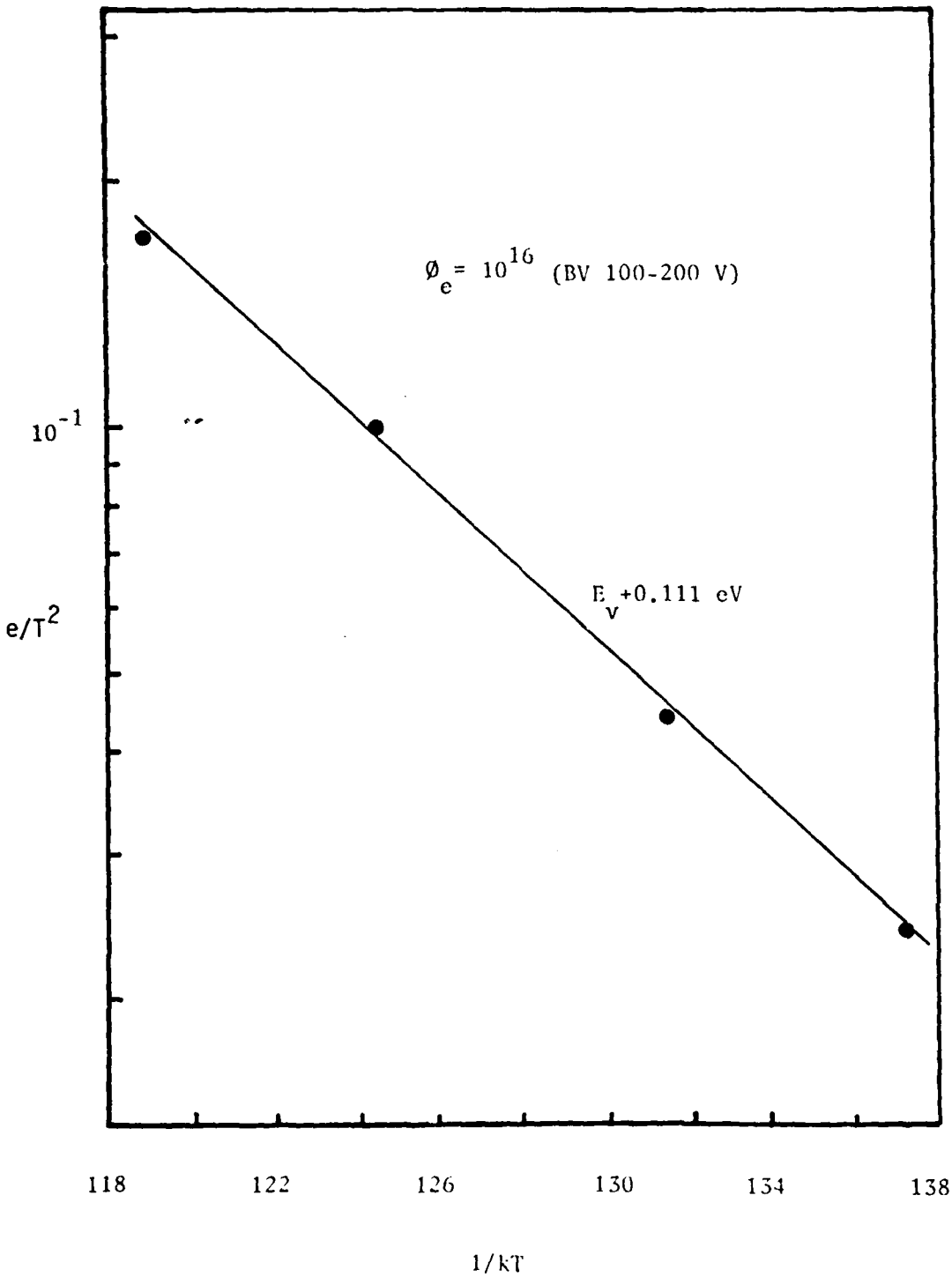

Fig. 3.29 Arrhenius plot of hole trap for Germanium irradiated by One-MeV electron.

Table 3.2 Defect-levels reported previously in irradiated Germanium.

(After Fan and Lark-Horovitz)

	Traps (eV)					
10 MeV Deutron	E_c-0.02	E_c-0.10	E_c-0.23	E_c=0.35	E_v+0.2	E_v+0.08
4.5 MeV Electron	E_c-0.01	E_c-0.10	E_c-0.24	E_c=0.35	E_v+0.22	E_v+0.10
Fast Neutron			E_c-0.2		E_v+0.18	E_v+0.07
Co^{60} gamma rays			E_c-0.2		E_v+0.26	

Table 3.1 Defect parameters in one-MeV electron irradiated germanium.

Samples	Φ_e (e/cm^2)	E_T (eV)	N_D (cm^{-3})	N_t (cm^{-3})	σ_n (cm^2)	σ_p (cm^2)	τ_n	τ_p	Defect origin
GE-A A=2.64*10^{-5}cm^2	0	E_c-0.257	2*10^{16}	2.33*10^{15}	3.56*10^{-14}		3.58*10^{-10}		Cu^{3-}
GE 23	10^{14}	E_c-0.237 E_v+0.174	1.82*10^{16}	1.24*10^{16} 4.89*10^{15}	3.8*10^{-14}	9.5*10^{-17}	6.30*10^{-9}	1.01*10^{-7}	VD_s Complex VVD_i Complex
GE22	10^{15}	E_c-0.268	1.87*10^{16}	1.34*10^{15}	6.47*10^{-14}		3.42*10^{-10}		VD_s Complex
GE21	10^{16}	E_c-0.208	1.65*10^{16}	4.90*10^{14}	5.82*10^{-14}		1.01*10^{-7}		VD_s Complex
GE-B A=2.66*10^{-5}cm^2	0	E_c-0.257 E_v+0.328	1*10^{15}	4.17*10^{14} 4.36*10^{14}	2.1*10^{-14}	2.18*10^{-12}	3.39*10^{-9}	4.94*10^{-11}	Cu^{3-} Cu^{3-}
GE13	10^{14}	E_c-0.237 E_v+0.103 E_v+0.160	7.45*10^{14}	4.12*10^{14} 4.07*10^{14} 1.40*10^{14}	1.08*10^{-14}	1.33*10^{-16} 5.9*10^{-16}	6.67*10^{-9}	8.67*10^{-7} 5.7*10^{-7}	VD_s Complex VVD_s Complex VVD_i Complex
GE12	10^{15}	E_c-0.268 E_v+0.256	8.9*10^{14}	5.29*10^{14} 3.2*10^{14}	1.56*10^{-13}	5.6*10^{-12}	3.59*10^{-10}	2.61*10^{-11}	VD_s Complex VVD_s Complex
GE11	10^{16}	E_c-0.238 E_v+0.111 E_v+0.169	7.46*10^{14}	4.10*10^{14} 2.97*10^{14} 2.57*10^{14}	3.75*10^{-14}	2.16*10^{-16} 5.94*10^{-16}	1.93*10^{-9}	7.31*10^{-7} 3.08*10^{-7}	VD_s Complex VVD_s Complex VVD_i Complex

formation of a secondary defect. The model is given by

$V + As_s \rightarrow As_sV$ ($E_c - 0.2$, $E_c - 0.24$ and $E_c - 0.27$ eV)

$VV + As_s \rightarrow As_sVV$ ($E_v + 0.10$ eV)

$VV + As_i \rightarrow As_iVV$ ($E_v + 0.17$ eV)

where As_i and As_s denote arsenic interstitial and arsenic substitutional site. Some of the irradiation-induced vacancies are trapped by impurity atoms forming the $E_c - 0.2$ eV level as the impurity-vacancy pair if the impurity is of group V. This is due to the fact that a negatively-ionized vacancy and a positively-ionized impurity of group V attracts each other easily. The other vacancies may be formed as the complex of divacancies. Hence these vacancies can be involved in the formation of the $E_v + 0.10$ and $E_v + 0.17$ eV levels. The $E_c - 0.2$ eV level is formed in the irradiated n-type germaniumm regardless of the impurity of group V. The shift of energy level between the $E_c - 0.2$ and $E_c - 0.3$ eV arises from different conditions of irradiation; that is, it results from the relaxation effect during annealing.

Based on the published report of Fukuoka et. at [Reference 3], it is concluded that the concentration of interstitial impurity by direct displacement of electron irradiation is much higher than that formed by the position exchange of self-interstitial with substitutional impurity. The higher fluence of electron irradiation causes the higher density of interstitial impurity but it decreases the density of substitutional impurity, and therefore reduces the possibility of forming a VVD_s (e.g. $E_v + 0.10$ eV) level. This is indeed the case for diodes GE 11 and GE 13. The total density of $E_v + 0.10$ and $E_v + 0.17$ eV is approximately equal to 5.5×10^{14} cm^{-3}. Thus, there might be a competition in the formation of two defect levels ($E_v + 0.10$ and $E_v + 0.17$ eV) in these irradiated diodes.

Radiation introduces Frenkel pairs i.e., vacancy interstitial pairs. It is assumed that no stable defects exist in the room temperature range which can be attributed to an isolated vacancy or an isolated interstitial in germanium.

In low-temperature irradiation experiment, the primary defect, a close vacancy-interstitial pair, requires the least energy for its formation [Reference 8].

In the irradiated germanium specimens, electron traps with energy of E_c- Ø.2, E_c- Ø.24, E_c- Ø.27, and hole traps with energy of E_v + Ø.1Ø, E_v + Ø.17 and E_v + Ø.26 eV levels were observed. The density of the E_c- Ø.2 eV (including the E_c- Ø.24 and E_c- Ø.27 eV) level is not dependent on the electron fluence but on the doping density. The defect parameters are listed in table 1, and the DLTS results are shown in Fig. 3.17 through Fig.3.39. The E_v+ Ø.17 eV hole trap, which is present only in the arsenic-doped germanium but not in antimony-doped germanium has not been reported previously. The origins of irradiation induced defects in germanium samples studied here are discussed as follows:

In germanium specimen irradiated by one MeV electrons, it seems that the secondary defects appear as a result of radiation-induced conversion of primary defects. These radiation-induced defects are capable of capturing two electrons in n-type germanium and are therefore double-acceptor centers.

In low-temperature surroundings, most displaced atoms easily lose their energies and therefore in high probability closely spaced double vacancies or divacancies probably associated with interstitials or impurity atoms can be formed. A negatively charged vacancy will migrate in the vicinity of a positively charged interstitial impurity.

In the case where defects such as VD_s, VVD_s and VVD_i are thought to be formed in parallel process, a divacancy exists and participates in the

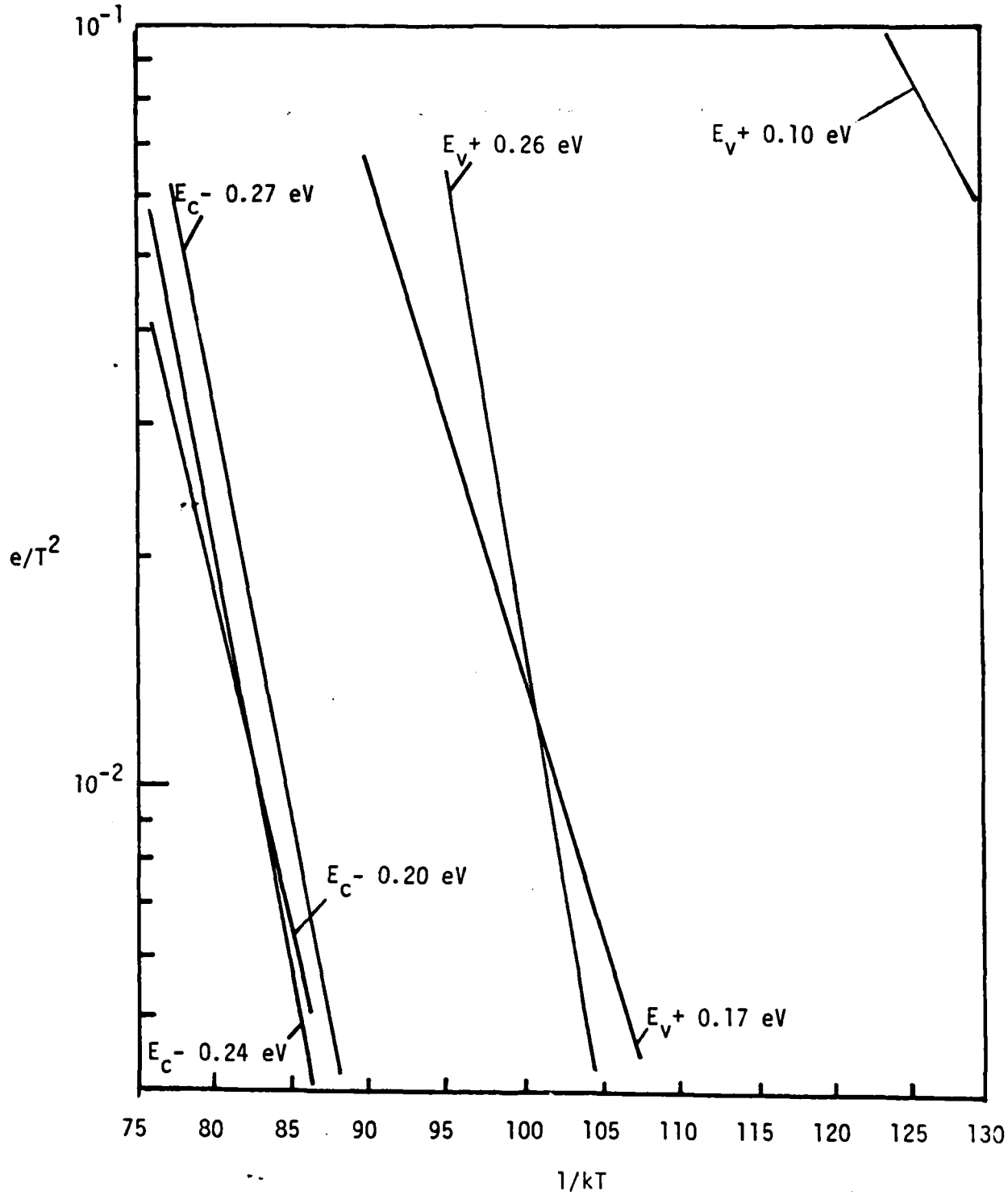

Fig. 3.39 Arrhenius plot of major traps of Germanium irradiated by One-MeV electron.

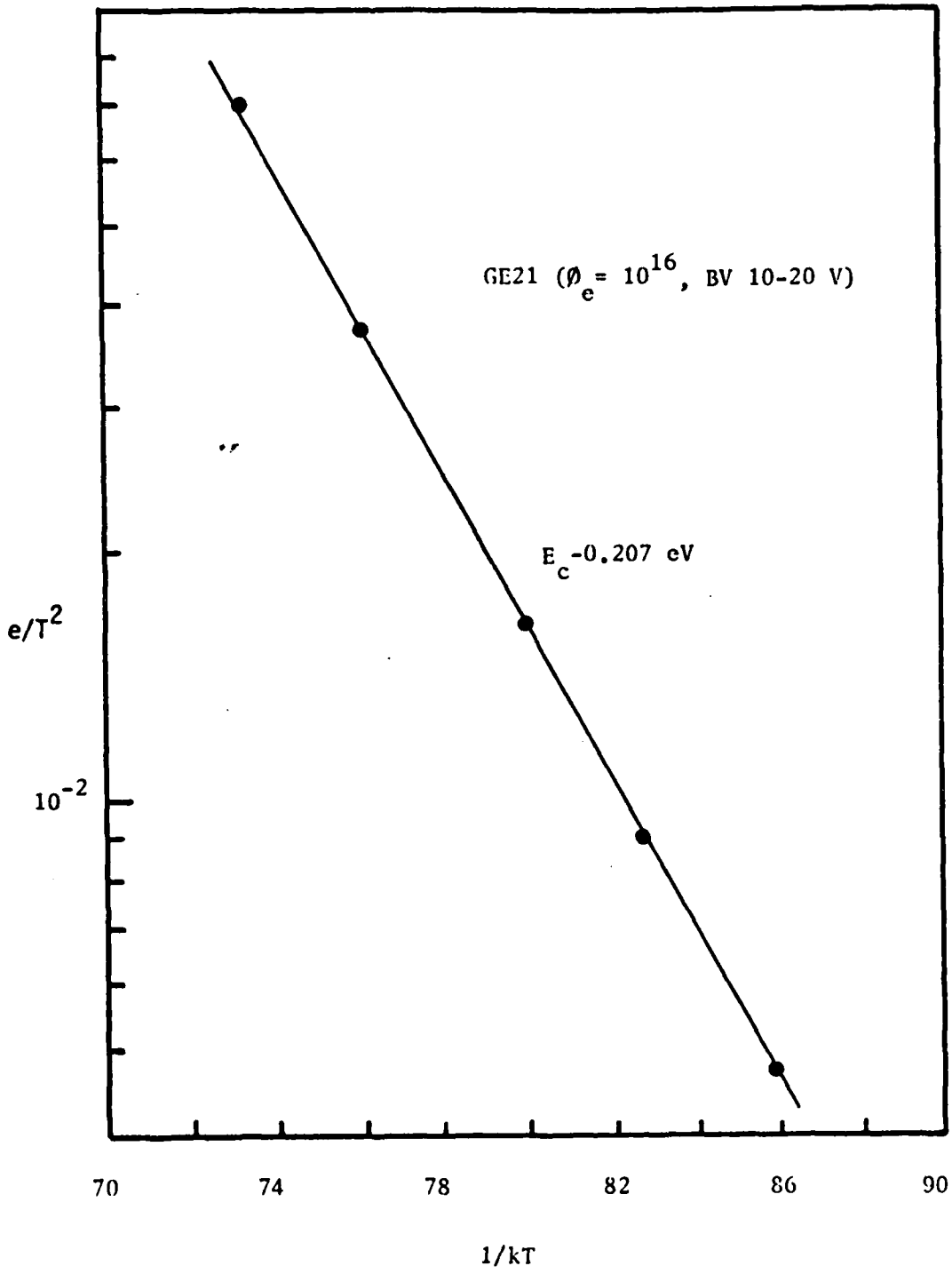

Fig. 3.38 Arrhenius plot of electron trap for Germanium irradiated by One-MeV electron.

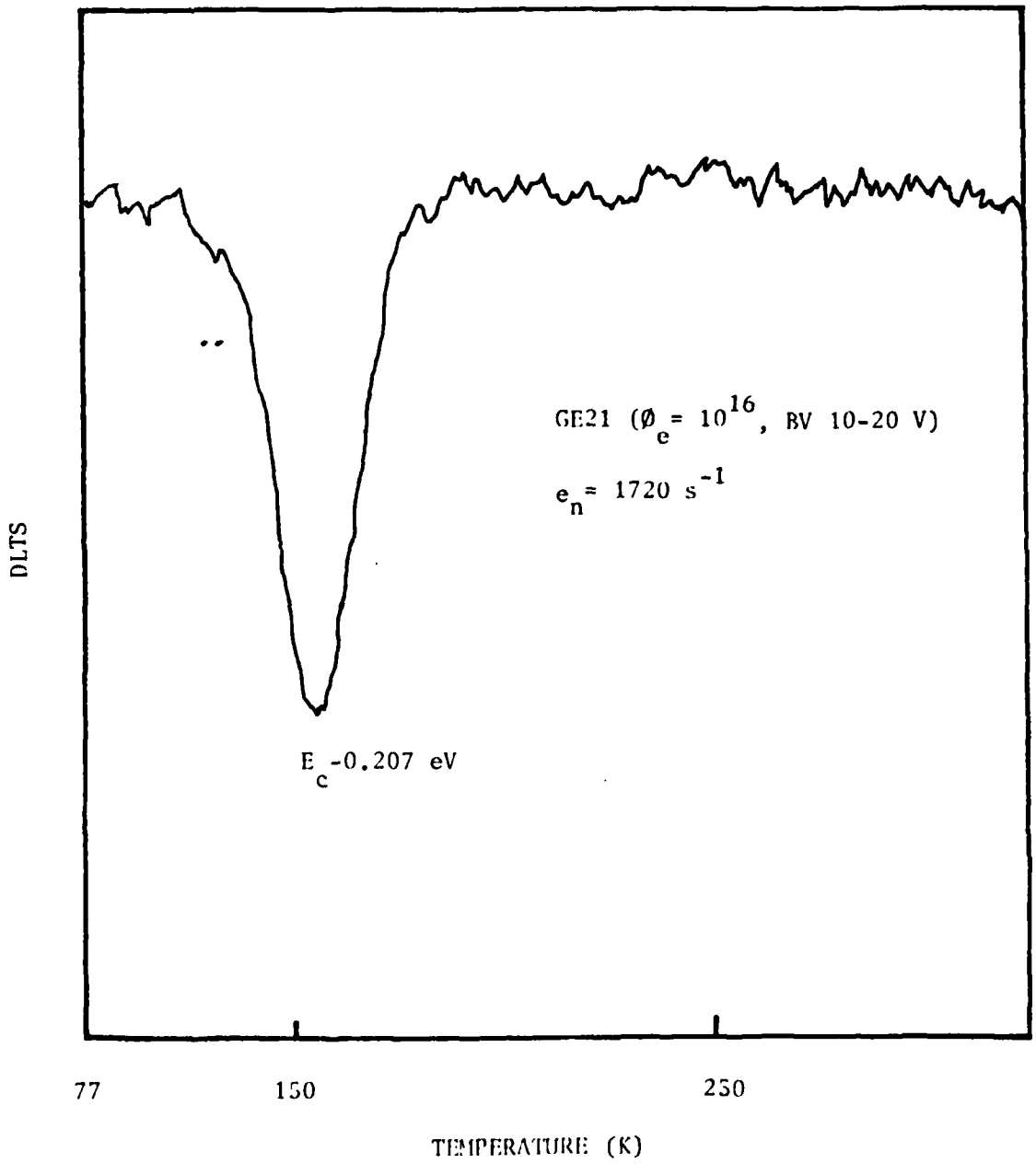

Fig. 3.37 DLTS scan of electron trap for Germanium irradiated by One-MeV electron.

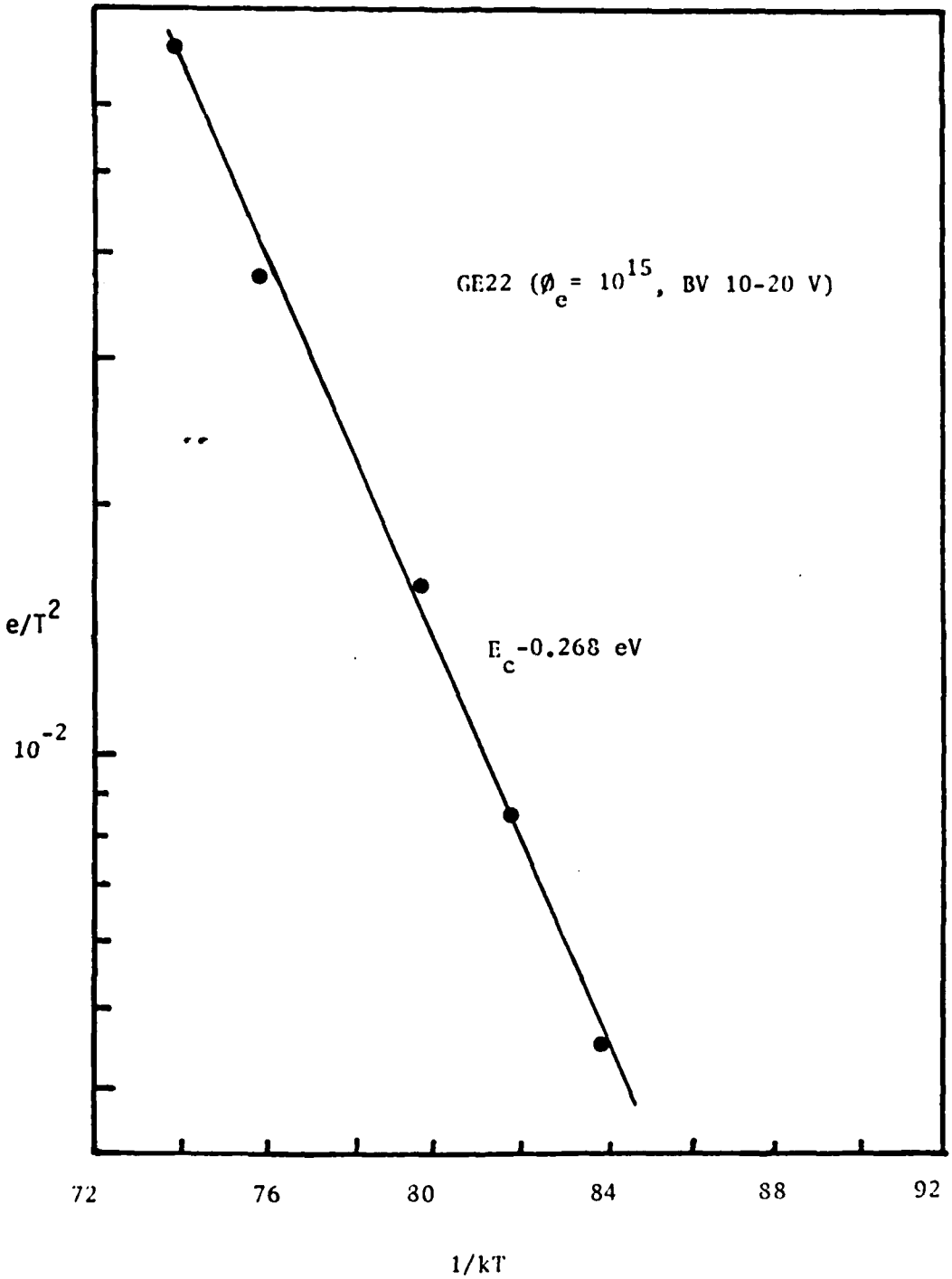

Fig. 3.36 Arrhenius plot of electron trap for Germanium irradiated by One-MeV electron.

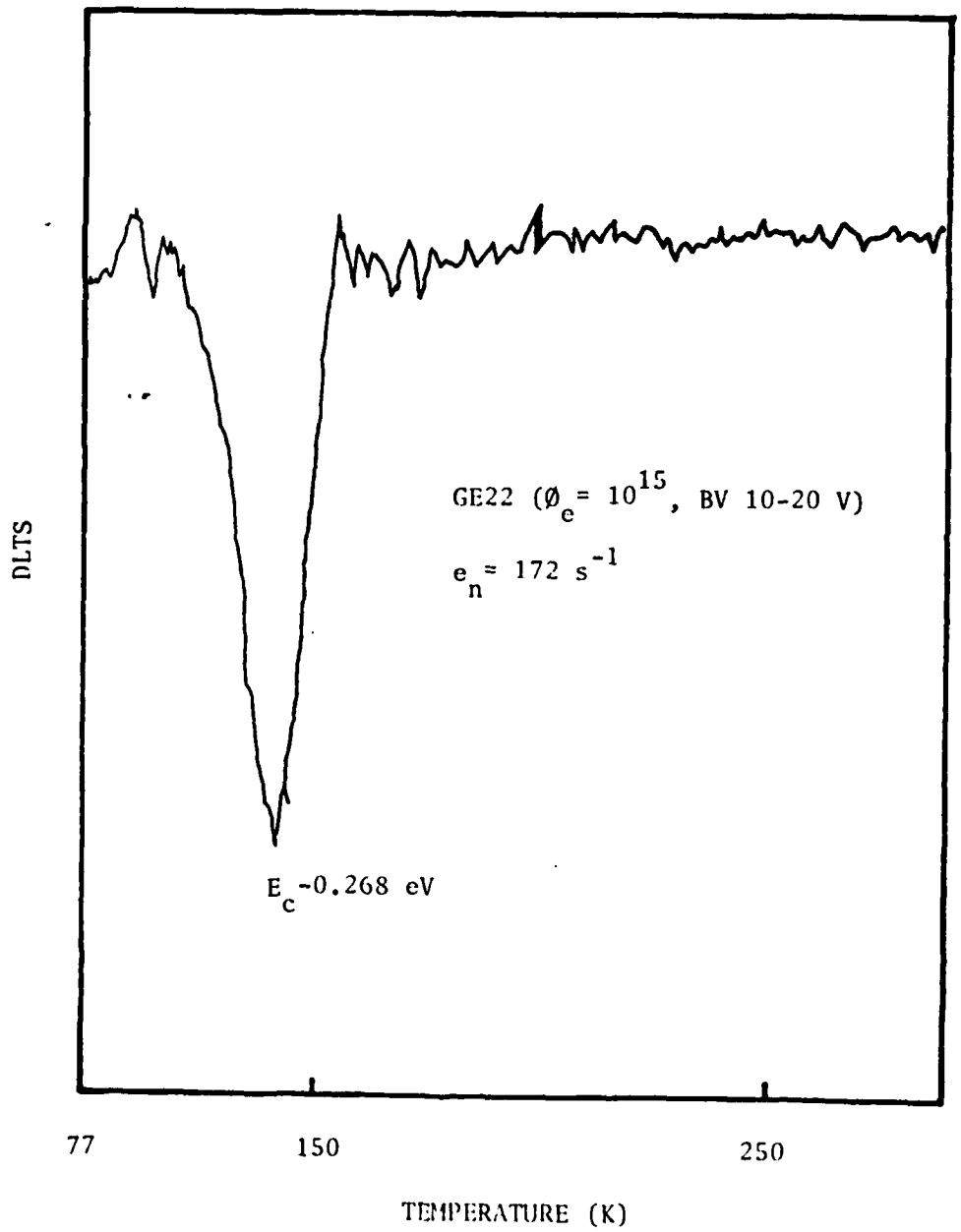

Fig. 3.35 DLTS scan of electron trap for Germanium irradiated by One-MeV electron.

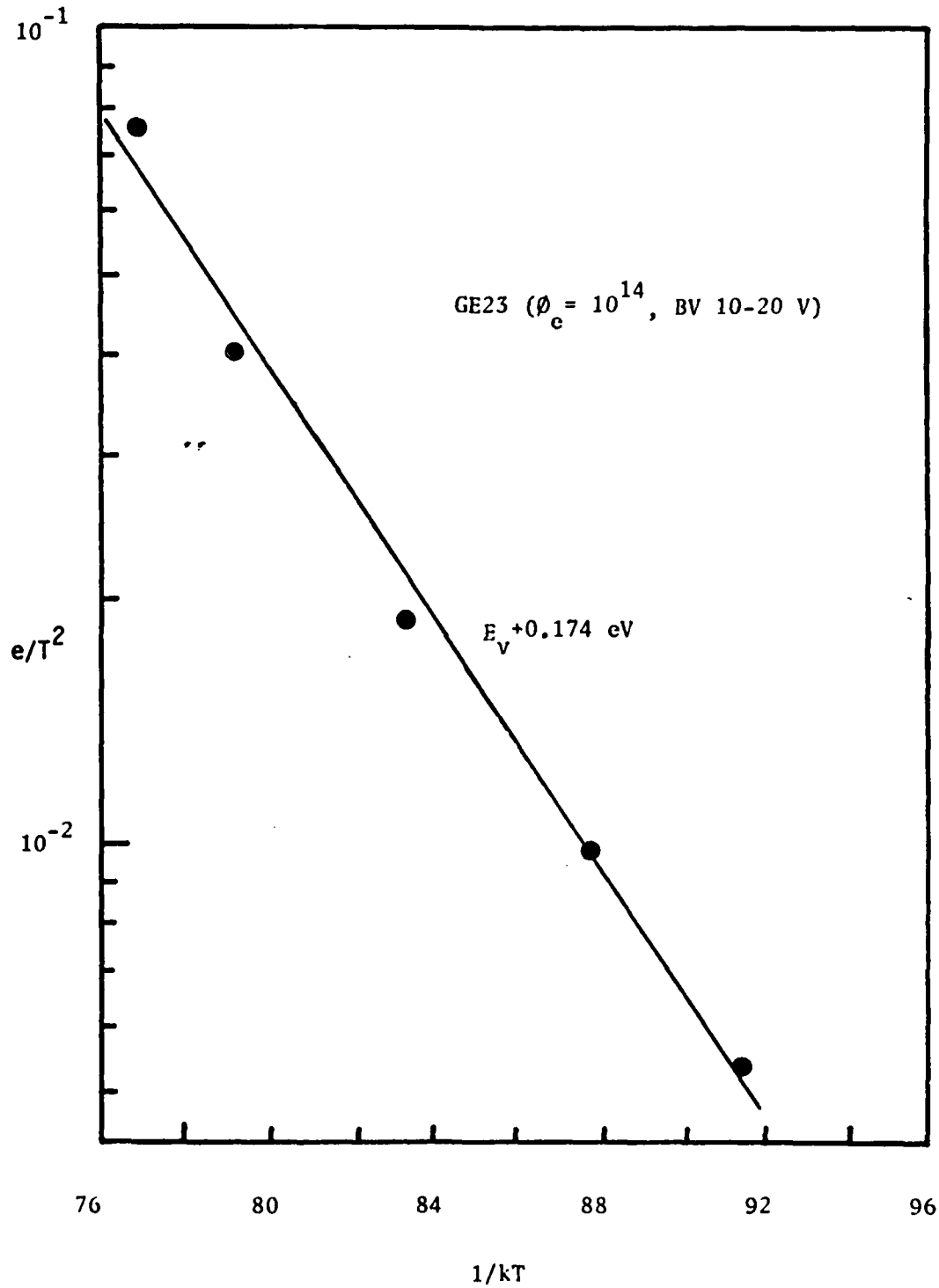

Fig. 3.34 Arrhenius plot of hole trap for Germanium irradiated by One-MeV electron.

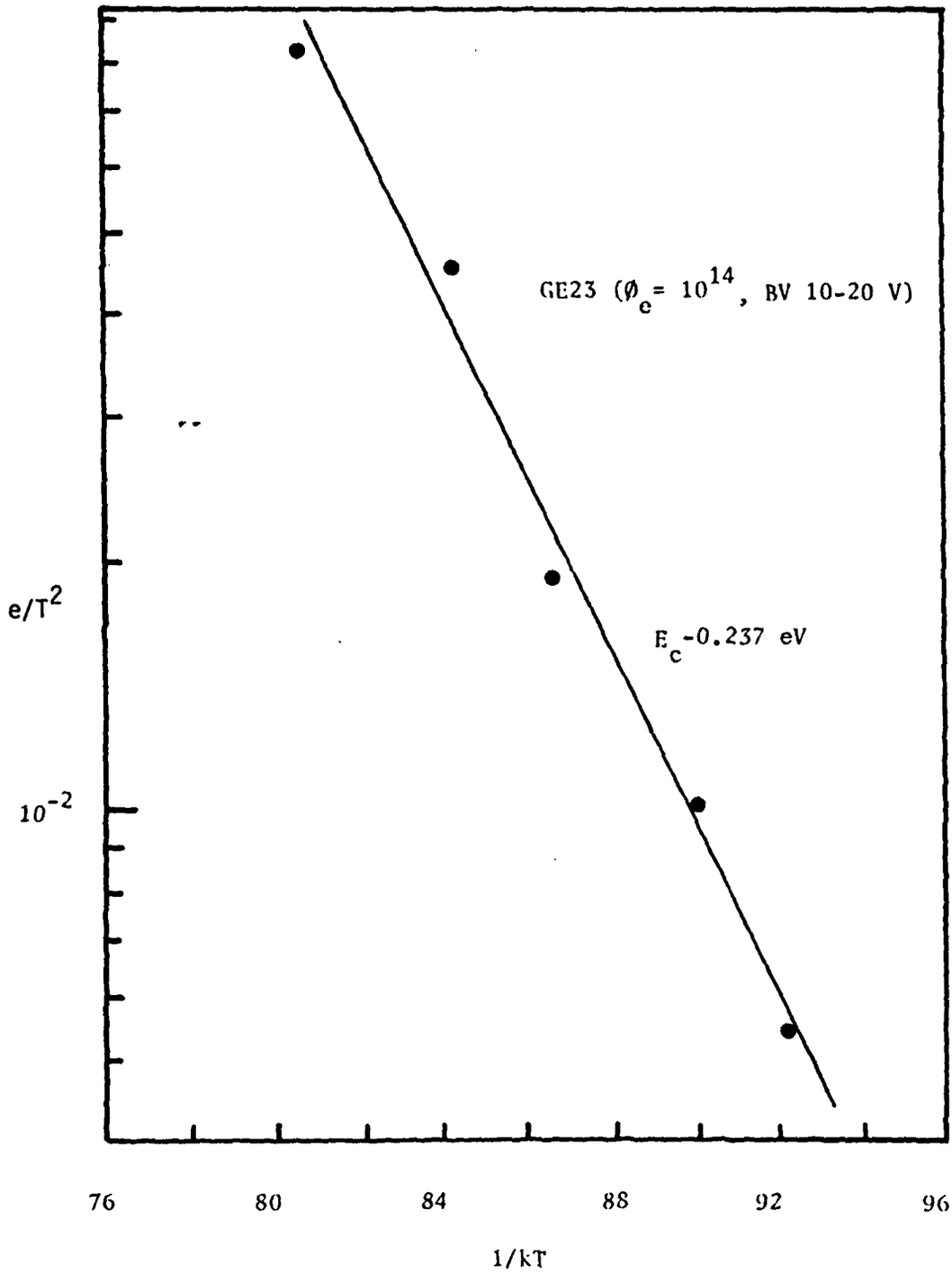

Fig. 3.33 Arrhenius plot of electron trap for Germanium irradiated by One-MeV electron.

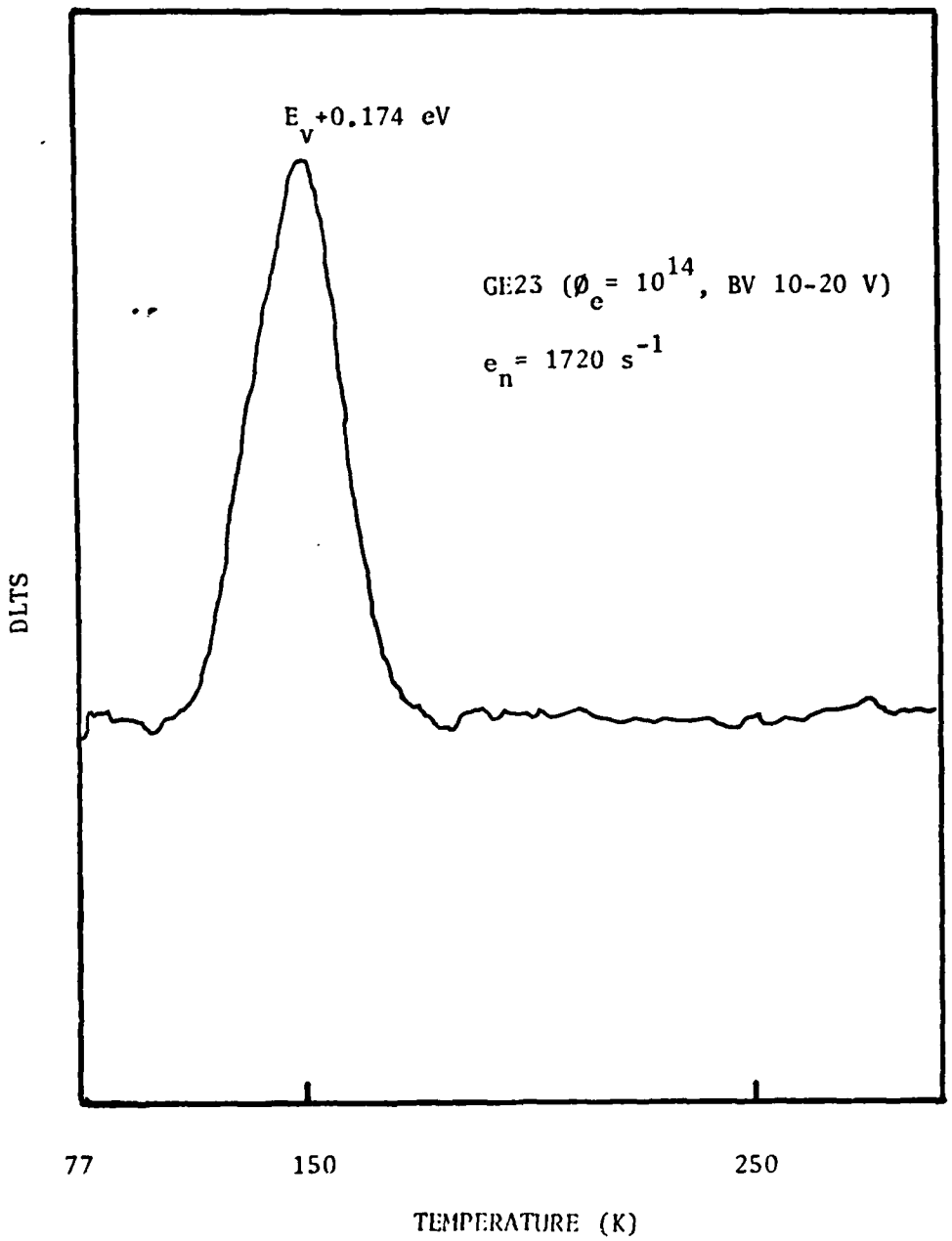

Fig. 3.32 DLTS scan of hole trap for Germanium irradiated by One-MeV electron.

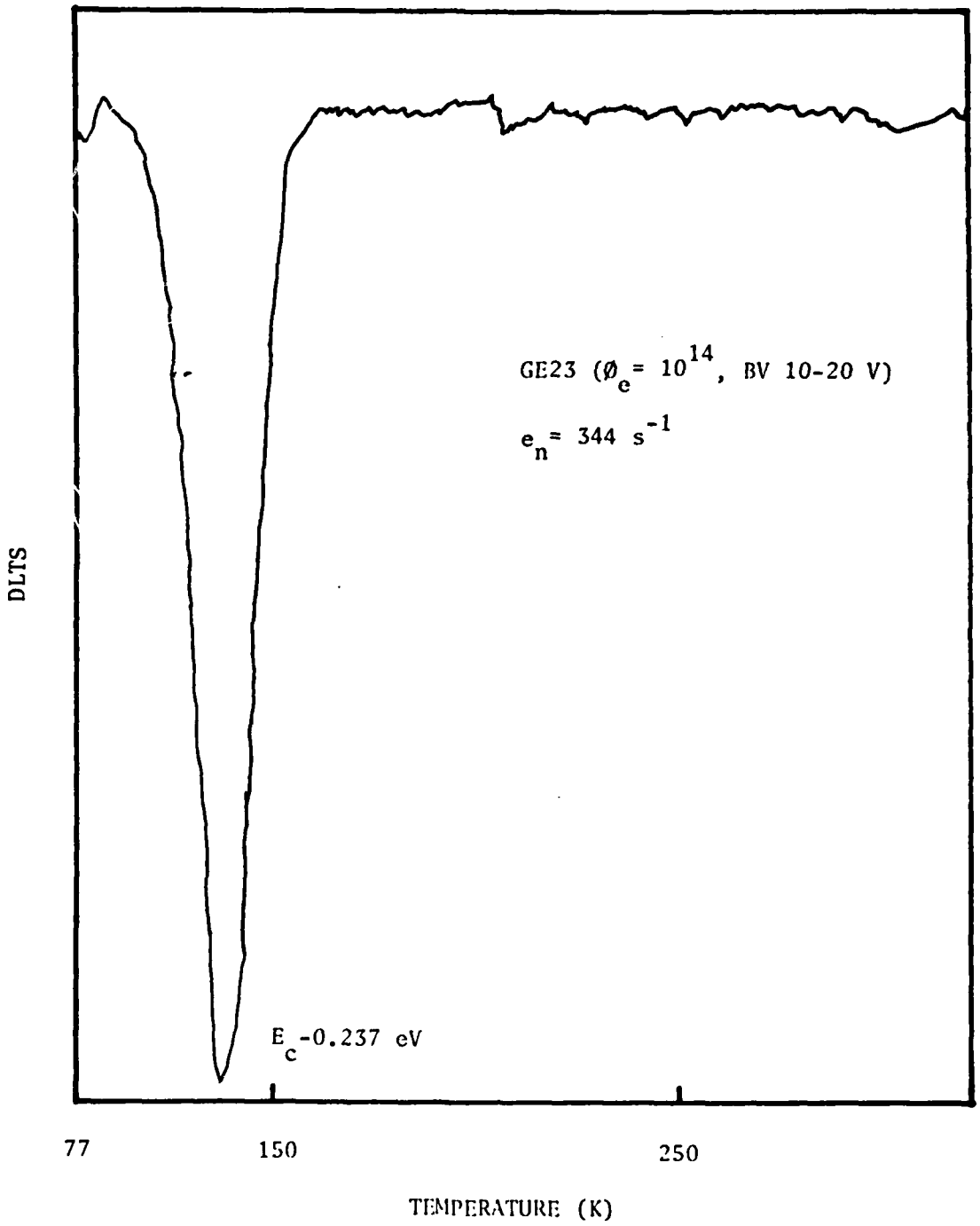

Fig. 3.31 DLTS scan of electron trap for Germanium irradiated by One-MeV electron.

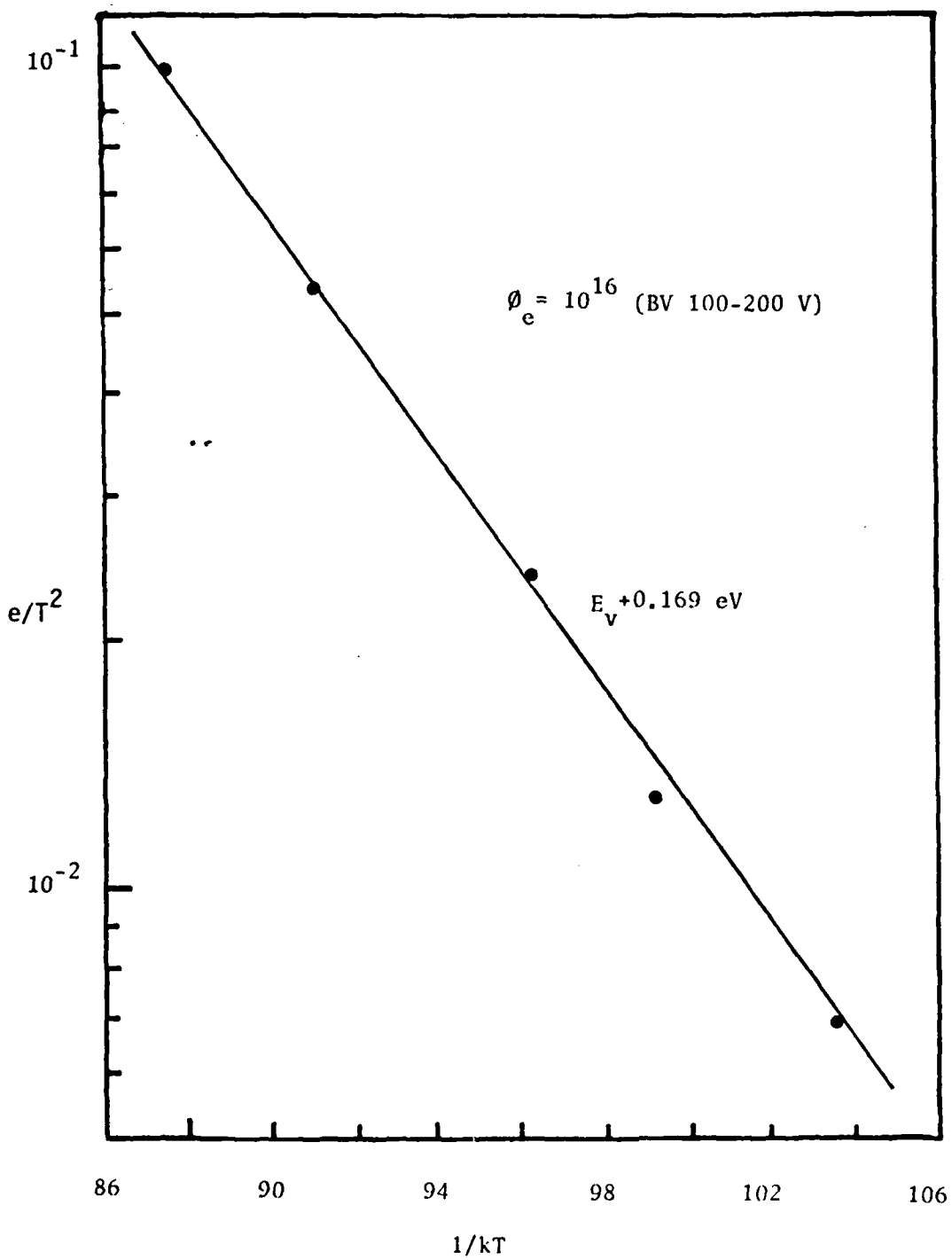

Fig. 3.30 Arrhenius plot of hole trap for Germanium irradiated by One-MeV electron.

Gerasimov et al. [References 9,10] reported that annealing in the temperature range 200-300 K increases the density of E_c - 0.24 eV while the density of deeper acceptor states decreases with increasing annealing temperature.

3.4 Summary

Electron irradiation introduces acceptor type states in germanium. These remove electrons from the conduction band in n-type germanium. In the n-type germanium irradiated by electron or gamma ray, the E_c- 0.2 and E_v+ x eV (below the midgap), whose value of x depends on the doping material, can be found (x = 0.10 for As and P, 0.12 for Sb, 0.16 for Bi). These two levels have essentially the same defect density.

The E_c- 0.2 eV, E_c- 0.24 eV, E_c- 0.27, E_v+ 0.10, E_v+ 0.17 and E_v+ 0.26 eV could be found from this experiment. Different fluences cause only the different relaxation conditions of defect and thus shifts of the energy level occur in the bandgap. Note that the introduction rate of defect concentration does not depend upon the fluence but on the impurity concentration. These defects cannot be attributed to isolated interstitials or isolated vacancies but to vacancy-impurity complexes or divacancy-impurity complexes.

The E_c- 0.24 eV and E_v+ 0.10 eV have essentially the same density. The origin of the E_v+ 0.17 eV is ascribed to a divacancy plus As interstial complex.

The defect introduction rate is independent of the fluence, although the different fluences can give different conditions for the formation of secondary defects that cause the shift of activation energy for the E_c- 0.2 level. Table 3.1 summarizes the results obtained from the DLTS analysis of the one-MeV electron irradiation induced defects in germanium specimen.

IV. Results of One-MeV Electron Irradiation in $Al_xGa_{1-x}As$

4.1 I-V Measurements

The I-V measurements were performed on $Al_xGa_{1-x}As$ p-n Junction cell with x=0.05 and x=0.17 and irradiated by one-MeV electrons with fluence of $\phi_e = 10^{15}$ and 10^{16} cm^{-3}. The result is shown Fig. 4.1. The recombination current component as given by Eq. (3-1), is larger in the sample irradiated with the fluence $\phi_e = 10^{16}$ cm^{-2} than the sample with $\phi_e = 10^{15}$. However, from the DLTS results, it is found that two electron traps, $E_c - 0.19$ eV and $E_c - 0.29$ eV, have comparable concentration independent of the fluence level. It is supported by the result of C-V measurement which shows higher carrier removal in the sample with higher fluence.

4.2 C-V Measurements

The background carrier density in the AlGaAs epilayer can be calculated from the C^{-2} vs voltage plot as described in section 3.1. The result of this calculation is summarized in table 4.1, along with the measured defect parameters.

4.3 DLTS Measurements

The DLTS measurement was performed on $Al_xGa_{1-x}As$ p-n junction cells with x=0.05 and x=0.17. The results show that no measurable deep-level defects exist in samples with x=0.05 and two electron traps with energies of $E_c - 0.19$ eV and $E_c - 0.29$ eV were observed in cells with x=0.17. Two trap levels have almost the same trap density independent of doping concentration and irradiation fluence.

Our observed electron traps are in good agreement with $E_c - 0.20$ eV and $E_c - 0.31$ eV reported by Lang[References 12-13]. These defects are the grown-in defects in that they exist in the unirradiated as well as irradiated samples, and were found to depend very little on the total fluence of

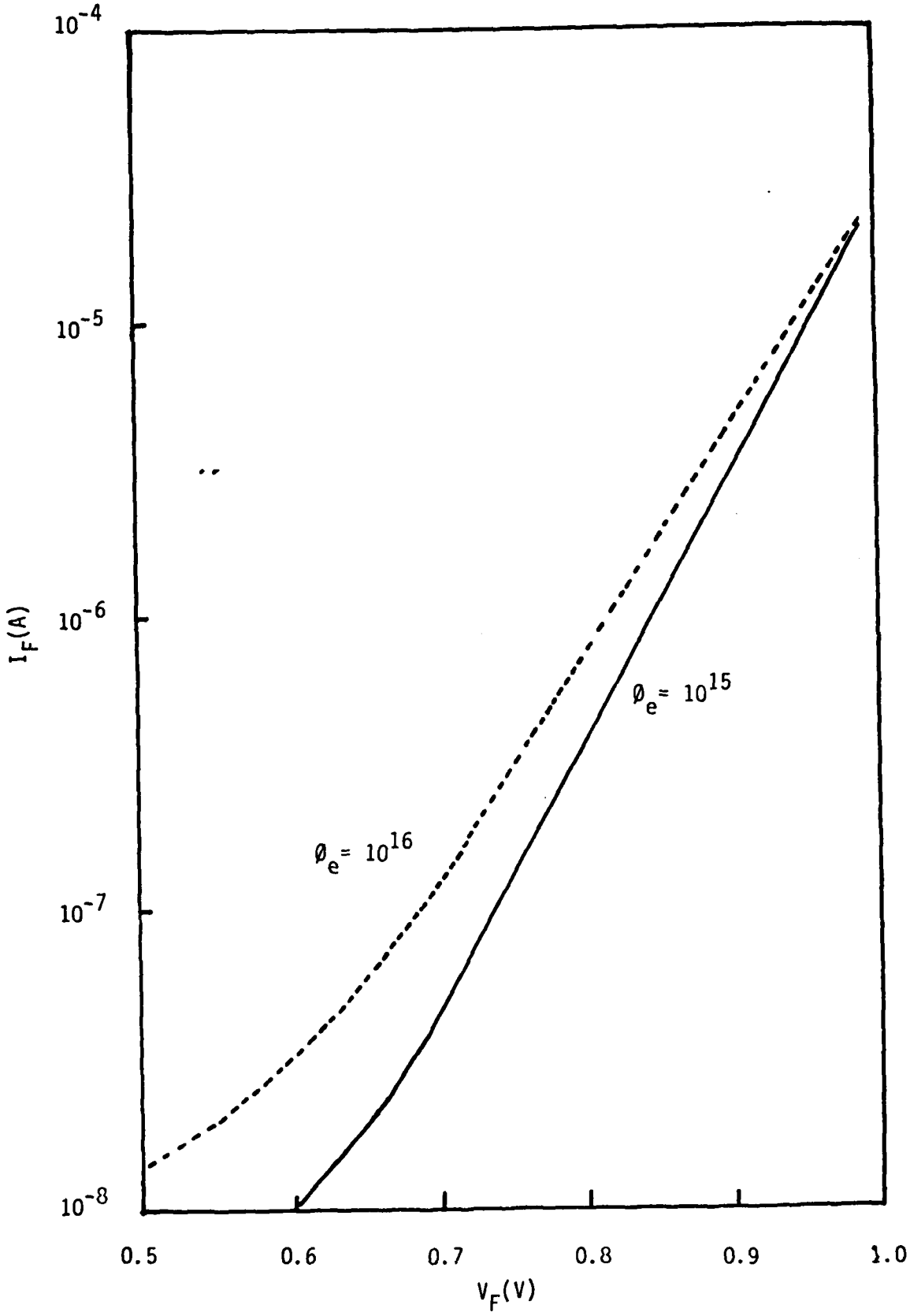

Fig. 4.1 Current vs forward -biased voltage for $Al_{0.17}Ga_{0.83}As$ irradiated by One-MeV electron.

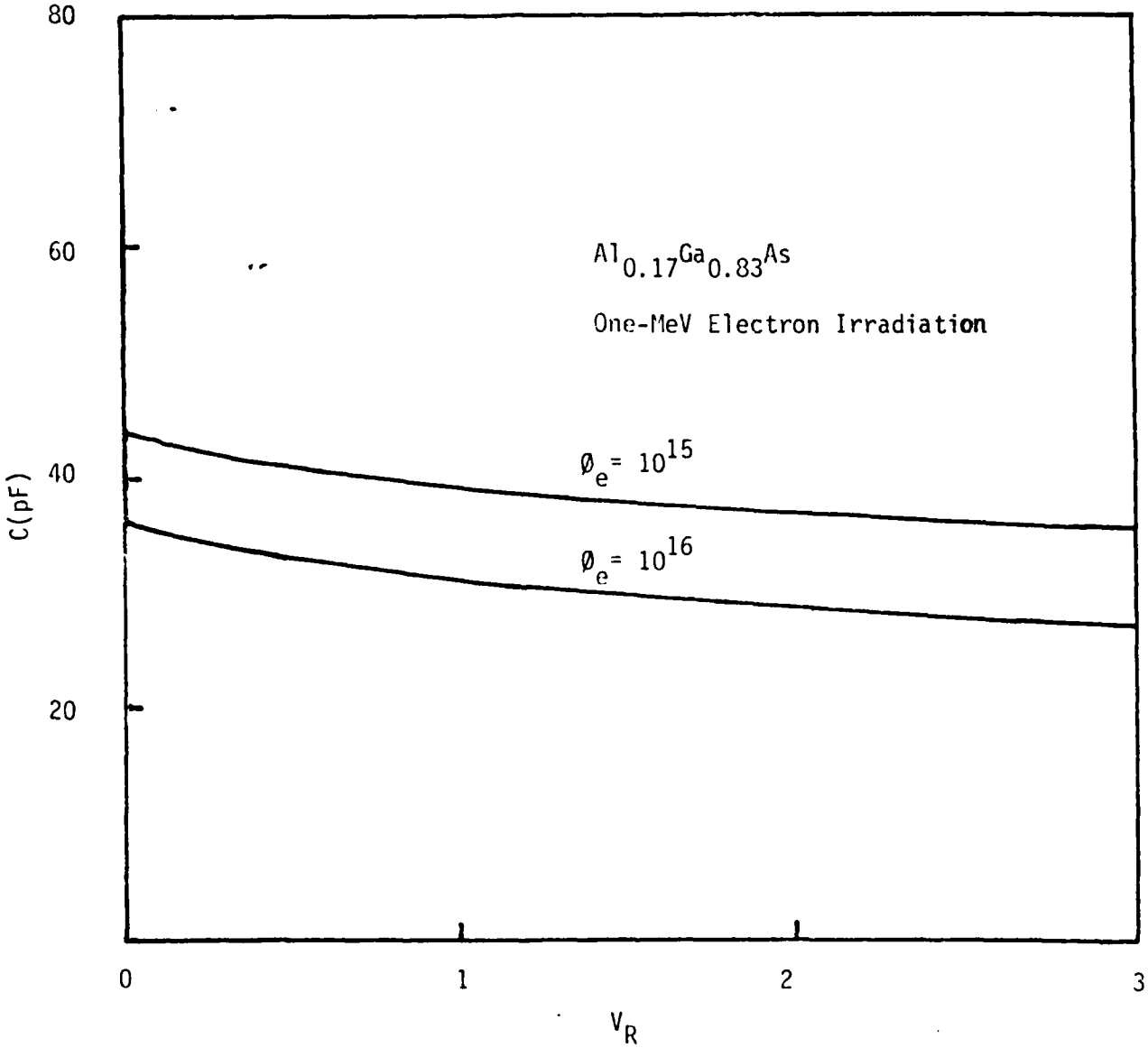

Fig. 4.2 Capacitance vs reverse-biased voltage for $Al_{0.17}Ga_{0.83}As$ irradiated by One-MeV electron.

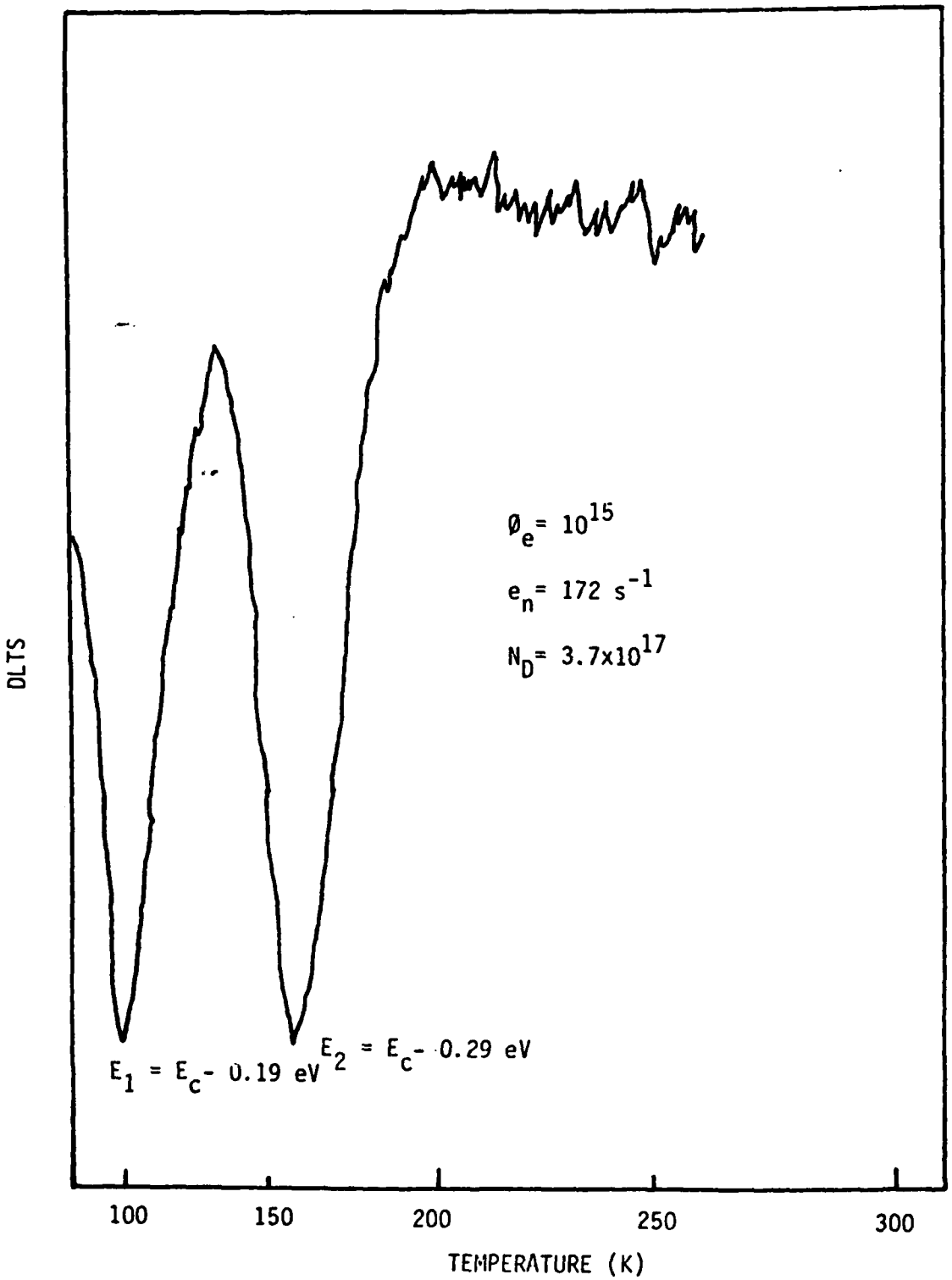

Fig. 4.3 DLTS scan of electron traps for $Al_{0.17}Ga_{0.83}As$ irradiated by One-MeV electron.

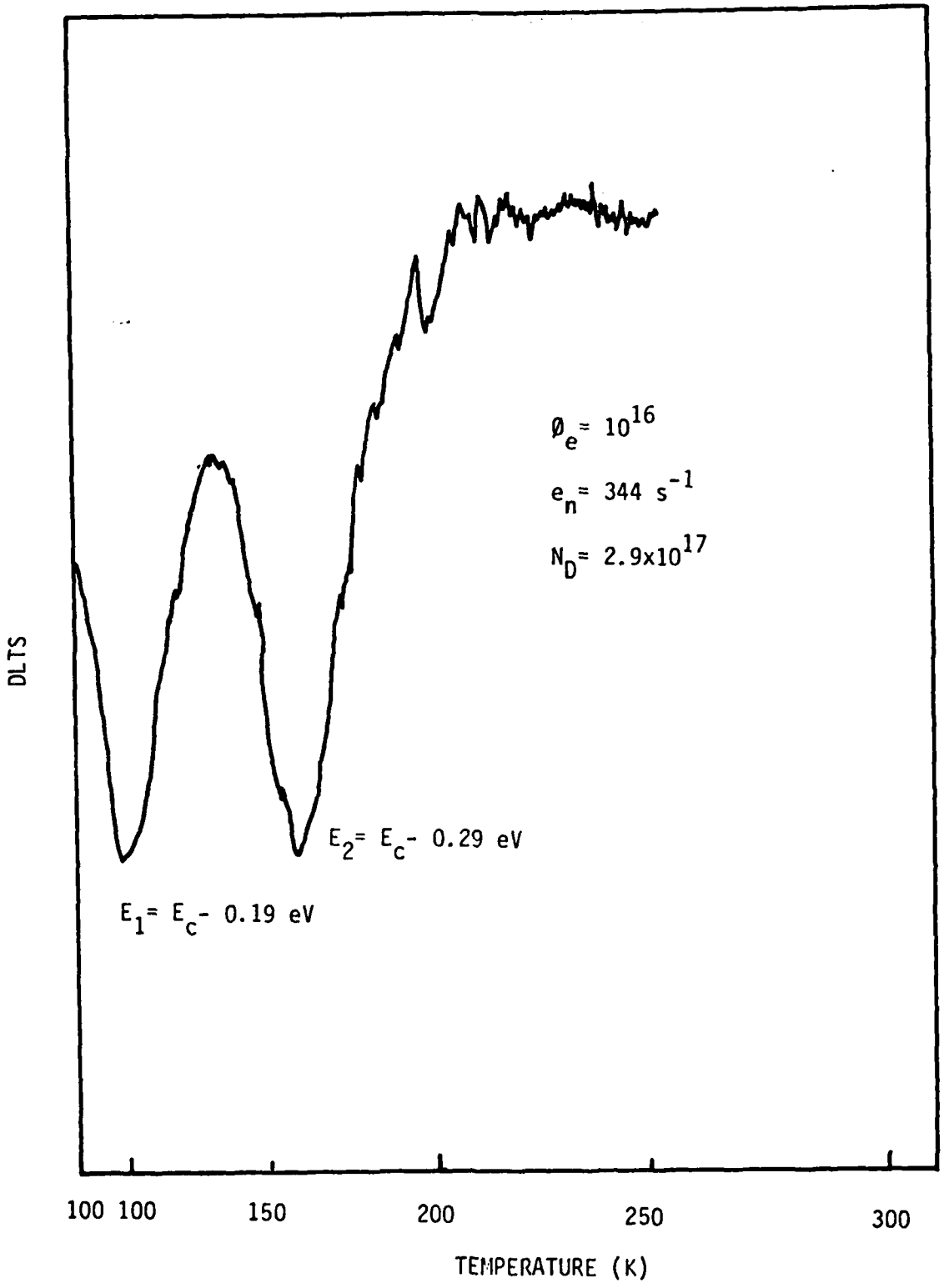

Fig. 4.4 DLTS scan of electron traps for $Al_{0.17}Ga_{0.83}As$ irradiated by One-MeV electron.

irradiation and the background doping density. From Lang's report[Reference 12], the energy vs aluminum fraction x is shown in Fig. 4.5. In irradiated Al_xGa_{1-x}, E1, E2, A and B levels are usually the observed defects. The origins of level A and B are unkown but they always exist in LPE $Al_xGa_{1-x}As$ in the direct bandgap range ($x < 0.36$). The E3 level is due to a vacancy since this level remains fixed relative to the valence band with x changed. The reason why these extra levels were not observed is not understood. More samples should be tried in the future.

Fig 4.3.1 shows the result of DLTS measurement and table 4.1 lists the defect parameters.

4.4 Summary

The reason why the E_c- 0.89 eV (which is a vacancy) was not observed in $Al_xGa_{1-x}As$ is not clear. Probably its concentration is too small compared with the E_c- 0.19 eV and E_c- 0.29 eV electron traps.

The E_c- 0.19 eV and E_c- 0.29 eV levels are grown-in defects, and are observed in samples with x=0.17 but not in cells with x=0.05.

V. Conclusions

In n-type germanium irradiated by one-MeV electrons, electron traps such as E_c-0.2, E_c- 0.24, E_c- 0.27 eV levels, and hole traps such as E_v+ 0.10, E_v+ 0.17 and E_v+0.26 eV were observed in these irradiated samples. The defect introduction rate is independent of the total fluence but is dependent on the density of doping impurity. None of them are attributed to a vacancy or an interstitial related defect. They are attributed to the vacancy + impurity complex related defects. One-MeV electron irradiation induces the acceptor-type defect levels around the E_c- 0.2 eV below the conduction band and another level below the midgap. These two levels have essentially the same trap density.

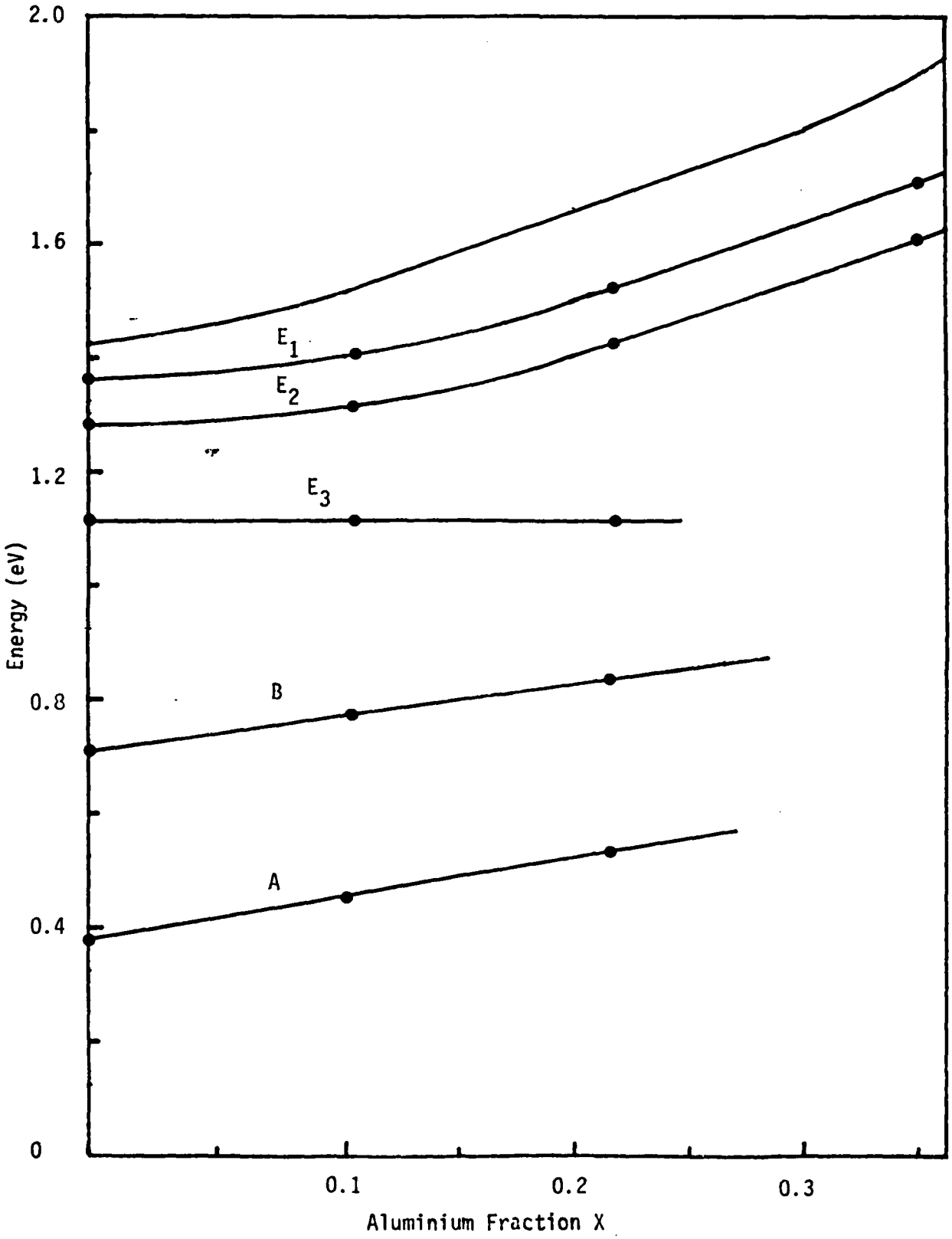

Fig. 4.5 Energy level shifts of deep levels in $Al_xGa_{1-x}As$ as a function Al mole fraction x.

Table 4.1 One-MeV Electron Irradiation Induced Defects in $Al_{0.17}Ga_{0.83}As$ Materials.

Electron Fluence (e/cm2)	N_d (cm-3)	E_T(eV)	N_T	σ_n (cm^2)
$\phi_e = 10^{15}$	3.7×10^{17}	$E_c - 0.19$	1.12×10^{16}	1.5×10^{-13}
		$E_c - 0.29$	1.3×10^{16}	2.7×10^{-14}
$\phi_e = 10^{16}$	2.9×10^{17}	$E_c - 0.19$	1.08×10^{16}	6.99×10^{-14}
		$E_c - 0.29$	1.13×10^{16}	5.14×10^{-14}

The E_v + 0.17 eV level is attributed to a divacancy-bismuth complex located at 0.16 eV above the valence band. However, it cannot be concluded that the E_v+ 0.17 level is associated with bismuth impurity. It is known that two acceptor-type levels, where one is above the midgap and the other is below midgap, have the same trap density. Thus, the sum of densities of the E_v+ 0.10 and E_v+ 0.17 eV should be less or equal than the density of the E_c- 0.24 eV under the assumption that the E_v+ 0.17 level is associated with bismuth impurity. This is not true from our present experiment. The sum of the densities of the E_v+ 0.10 eV and the E_v+ 0.17 eV is in fact exceeding the density of the E_c- 0.24 eV. This is unreasonable since it contradicts to the fact that annealing of the deeper acceptor levels increases the concentration of the E_c- 0.24 eV level in the temperature range from 200-300 K. Therefore it can be concluded that the E_c+ 0.17 eV level is a divacancy + interstitial arsenic complex.

In short, germanium cells show strong radiation hard characteristics, and should be suitable for use as a bottom cell material for cascade solar cell applications.

In $Al_xGa_{1-x}As$ with x = 0.05 and 0.17 irradiated by one-MeV electron, only the E_c- 0.19 and E_c- 0.29 eV were observed in cells with x = 0.17. None were found in $Al_{0.05}Ga_{0.95}As$. Since these two levels are independent of the electron fluence and background carrier concentrations they are grown-in defects. The effect of one-MeV irradiation on the deep-level defects in AlGaAs material is to cause some increase in the density of the two native defects observed in the as grown samples while no new deep-level defects were found in the AlGaAs materials by electron irradiation.

VI. References

1. J. C. Pigg and J. H. Crawford Jr. Phy. Rev. Vol.135, No.4A, p. A1141 (1964).
2. O. I. Curtis, Jr., and J. H. Crawford, Jr., Phy. Rev. Vol.124 No.6 p.1731 (1961).
3. N. Fukuoka, H. Saito and Y. Tatsumi, Inst. Phys. Conf. Ser.No.23 p.206 (1975).
4. T. V. Mashovets Inst. Phys. Conf. Ser.No.31 p.30 (1977).
5. S. N. Abdurakhmanova, T. N. Dostkhodzhaev, V. V. Emtsev, and T. V. Mahovets, Sov. Phys. Semicond. Vol.8 No.9, p.1144 (1975).
6. Y. Bamba, S. Tatsuta, T. Sakura and H. Hashimoto Inst. Phys. Conf. Ser.No.59, p.193 (1981).
7. T. A. Callcott and J. W. Mackay, Phys. Rev., Vol.161 No.3, 15, (1967).
8. S. N. Abdurakhmanova, T. Dostkhodzhaev and T. V. Mashovets, Soviet Phys. Semicond., vol.7, p. 1229, (1974).
9. A. B. Gerasimov, N. D. Solidze, N. G. Kakhidze, and B. M. Konovalenko Radiation Physics of Nonmetallic Crystals and P-P junction, edited by Minsk, P.65 (1972).
10. A. B. Gerasimov. N. D. Dolidze, K. I. Kasparyan, N. G. Konovalenko and M. G. Mtskhvetadze Soviet Physics-Semiconductors Vol.6 No.8, p.1368, (1973).
11. S. M. Sze, "Physics of Semiconductor Devices", 2ndedition, Wiley (1982).
12. D. V. Lang and R. A. Logan, Inst. Phys. Conf. Ser. No.43, p.433, (1979).
13. D. V. Lang, Inst. Phys. Conf., Ser. No.31, P.70 (1977).

VII. Publications and Confernce Presentations

1. W. L. Wang and S. S. Li, "One-MeV Electron and Low Energy Proton Irradiation Induced Defects in GaAs and $Al_xGa_{1-x}As$ Solar Cells," paper presented at the 17th IEEE Photovoltaic Specialists Conference," Orlando, FL., May 1-4 (1984).

2. W. L. Wang and S. S. Li, "Determination of Potential Well and Modelling of the Deep-Level Defects in GaAs,", paper presented at the 1984 International Electron Devices and Materials Symposium, Hsinchu, Taiwan, September 4-6 (1984). Paper appeared in the Proc. of the conference, pp.65-70.

3. W. L. Wang and S. S. Li,"Modelling and New Interpretation of the EL2 Electron Trap in GaAs," paper presented at the 16th International Conference on Solid State Devices and Materials," Kobe, Japan, August 30 - September 1, 1984.

4. S. S. Li and C. G. Choi, "DLTS Analysis of Deep-Level Traps in One-MeV Electron Irradiated Germanium," Solid State Electronics, to be published (1985).

☆U.S.Government Printing Office: 1985 — 559-065/20946

END

FILMED

11-85

DTIC